Energy Strategy Reviews 51 (2024) 101310

Contents lists available at ScienceDirect

Energy Strategy Reviews

journal homepage: www.elsevier.com/locate/esr

Systematic indoor experimental practices for simulating and investigating dust deposition effects on photovoltaic surfaces: A review

Abubaker Younis [a,*], Petru Adrian Cotfas [a], Daniel Tudor Cotfas [a]

[a] Electronics and Computers Department, Transilvania University of Brașov, Romania

ARTICLE INFO

Handling editor: Mark Howells

Keywords:
Photovoltaic performance
Dust soiling
Dust deposition density
Dust removal
Solar energy
Renewable energy

ABSTRACT

Dust accumulation can degrade the performance of a photovoltaic (PV) cell to varying degrees that are directly proportional to the deposition density. The comprehensive review presented here categorizes and describes the laboratory-based experimental practices interested in studying the effect of dust accumulation on PV modules or surfaces and then seamlessly analyzes and interprets the information extracted from the reviewed literature. Hence, the key findings of this article, which simultaneously represent its applicable added values, are a deduced pattern from the relevant research that can be generalized to all types of similar future studies. This methodical arrangement begins with dust sampling and physio-chemical characterization. This step is followed by a manual or automated scattering of dust inside the test chamber or on top of the test bench to fall on the deposition surface, after which the electrical, thermal, optical, and dust removal characterizations are carried out. The second chief outcome is an inclusive list of all the equipment used in the different workflow stages. The most significant recommendation drawn from this effort is that it is necessary to develop a protocol that allows benefiting from the mature experimental practices with valid results to include them in endurance and reliability tests for PV panels in the relevant international standards.

1. Introduction

The global transition towards renewables to secure the energy demand is an adaptation strategy driven by the fundamental vulnerability of the world to climate change. Solar energy, especially Photovoltaic (PV), is gaining a magnificently increasing role in the global energy mix. For instance, China has around 400,000 MW_p installed capacity of solar PV generators [1], accounting for 3 % of the total production of this global energy giant [2]. Also, Germany has Europe's most installed PV capacity, contributing 8 % to the country's power production [3]. Therefore, any improvement in the efficacy of electric current generation at a single solar cell level will eventually have attractive economic outcomes in multi-megawatt solar PV projects. A recently promoted topic concerning this enhancement is presenting the scrutiny of the dust deposition effects in a standard manner [4,5], enabling us to estimate the decrease in the productivity of PV panels location-wise.

The dust, defined as solid particles less than 500 μm [6], which is suspended in the atmosphere by sizes smaller than 1–100 μm [7], has undebatable consequences on solar PV performance, mainly its sediments on the panel surface [8]. An excellent quick example is the work done by Juaidi et al., who obtained 9.99 % power loss from a polycrystalline silicon (poly-Si) PV system kept unclean or dusty for seven months [9]. The physical explanation of this power loss is that the particles settling on the surface mesh together, diffusing solar rays from reaching the PV cells and cutting short the amount of transmitted light [10]. For instance, Mastekbayeva and Kumar found that one month of accumulated dust (or 3.72 g/m^2) reduced the glazing transmittance by 14 %, ultimately causing a significant loss in the produced electric power [11]. If we look deeper into the physics behind the dust sticking to the PV surfaces, the main adhesion forces that will be noticed are capillary, electrostatic, and van der Waals, all considered inter-particle forces mainly driven by the small diameter of the particles (less than 1 μm). In a close fashion, the deposition and clinging of the larger dust fragments (less than 5 μm) is caused by gravitational and inertial forces, making the coarse grains less likely to settle than the finer ones [12,13]. Fig. 1 illustrates the typical dust particle adhesion forces [14,15]. It needs to be said that the van der Waals and electrostatic forces are highly active during the dry deposition mechanism, whereas all forces are active during the wet deposition mechanism [15].

Technically speaking, the dust build-up causes meaningful degradation in the short-circuit current (I_{sc}) [16], that its magnitude depends

* Corresponding author.
E-mail addresses: a.younis@imresearch.sd, abubaker.younis@student.unitbv.ro (A. Younis).

https://doi.org/10.1016/j.esr.2024.101310
Received 11 September 2023; Received in revised form 22 November 2023; Accepted 10 January 2024
Available online 25 January 2024

List of abbreviations

a-Si	Amorphous silicon
CCD	Charge-coupled device
EDX or EDS	Energy-dispersive X-ray spectroscopy
I_{sc}	Short-circuit current
I – V	Current-voltage characteristics
Mono-Si	Monocrystalline silicon
Poly-Si	Polycrystalline silicon
PV	Photovoltaic
RTD	Resistance Temperature Detector
SEM	Scanning electron microscope
XRD	X-ray diffraction
XRF	X-ray fluorescence

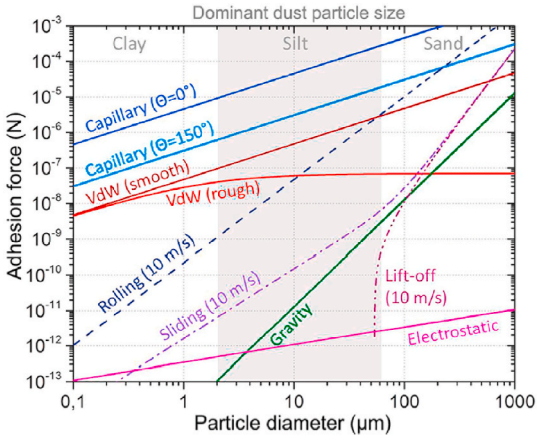

Fig. 1. Typical dust particle adhesion forces [14,15].

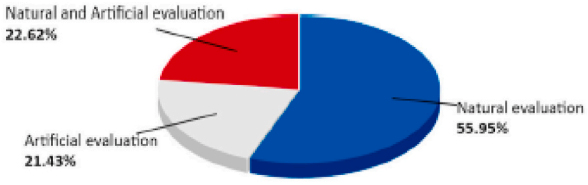

Fig. 2. Share of literature studies based on the deposition technique [30].

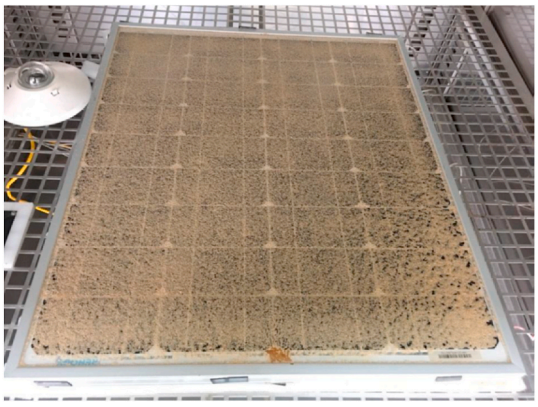

Fig. 3. Uniformly distributed plaster soil within an indoor experimental setup [37].

on the dust material and characteristics [8]. In a typical case, El-Shobokshy and Hussein obtained an 82 % reduction in I_{sc} after artificially accumulating dust reached 250 g/m^2 [17]. Moreover, Tripathi et al. reassured that the loss in I_{sc} increases as the particle size decreases [18]. They obtained a 15.68 % loss corresponding to 600–850 μm and 49.01 % associated with less than 75 μm. As if there is no limit to the adverse effects of dust on PV performance, its agglomeration will hamper heat dissipation, potentially forming a temperature gradient and disturbing the solar cell's conversion efficiency or causing physical damage to the PV structure [19,20]. Not forgetting that other environmental conditions like humidity, wind, and temperature can contribute to the performance loss process, which scales up the wastage to 80 % in certain desert areas [21]. Al Siyabi et al. investigated the effect of dust-soiling on a 2 MW_p PV system installed in a car park and noticed that a soiling percentage of 7.5 % reduced the monthly electricity generation by 5.6 % [22]. Also, Ammari et al. presented their results benefitting from one-year data of outdoor experiments conducted on poly-Si modules under semi-arid weather and recorded a 15 % daily reduction in the electrical output due to dust presence [23]. Additionally, Asad Ullah et al. reported average daily power losses of 1.11 % at 0° and 0.11 % at 90° due to 120 days of outdoor dust accumulation tests corresponding to variable tilt angles [24].

Continuing our critical overview, dust gatherings on top of the PV module have the convenience of being uniformly or non-uniformly dispersed under outdoor conditions considering the site characteristics, dust properties, wind speed, ambient temperature and humidity, tilt angle, module dimensions, and surface material properties [25]. The distribution uniformity solely affects the I_{sc} of the solar cell or module, a consequence associated with the shading phenomenon and spectral transmittance losses that, in principle, lower the electrical current [26]. From this perspective, the review paper written by Zaihidee et al. revealed that an amount of 20 g/m^2 of accumulated dust could deteriorate the I_{sc} of a PV panel by 15–21 %, eventually interrupting the solar generator yield [20]. An additional effort executed by Chanchangi et al., which was based on a 1.5 W mini-module with two different surface materials (i.e., Acrylic plastic and low iron glass) placed in an indoor setup, quantified the reduction in I_{sc} made by dry and wet soiling mechanisms of clay soil. Deterioration percentages of 33 % and 14 % corresponded to the dry deposition, while 96 % and 93 % related to the wet deposition for the acrylic plastic and glass surfaces, respectively [27]. In a different work, the team of Chanchangi et al. analyzed outdoor collected data from an urban PV system and discovered a 73 % decrease in I_{sc} coming out of the amorphous silicon (a-Si) module and at least a 65 % decrease out of the crystalline silicon panels over one year and seventeen months of absolute no cleaning, respectively [28].

Location-wise, dust significantly affects PV performance in the humid, arid, and desert climate, the harsh conditions mainly found in the Middle East and North Africa [29]. On the other hand, there is less potential for natural dust generation in Europe, especially when compared to arid and semi-arid places [30]. For example, the experimental research conducted in Poland by Jaszczur et al. reported a 2.1 % efficiency loss caused by 480 mg of dust accumulated mass over one week [31]. But if we considered Iran, for instance, the dust deposition density could reach 10 gm^{-2}, responsible for a 15–60 % power drop, as reported by Gholami et al. [32]. A second example is from Sudan, where the dust deposition density is nine times greater than in the UK [29]. In the tropical climate of India, Lakshmi and Ramadas investigated the effect of four different dust materials available in the local vicinity of Chennai and found that coal caused the worst power loss by 73.51 % [33]. In Brazil, Fraga et al. assessed the impact of dust on a solar power plant in a stadium at Minas Gerais to reveal a 13.7 % loss in peak power after 23 days of exposure [34]. In California, Mejia and Kleissl quantified the dust deposition effect to be 0.051 % per day loss of the conversion efficiency [35].

Based on the literature, the outdoor experimental studies dominate

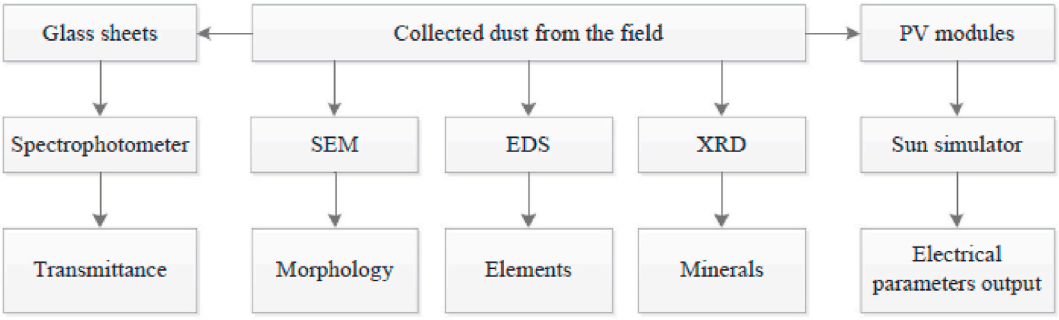

Fig. 4. Frequent indoor dust soiling research pattern [41].

the content related to the simulation of dust deposition on PV surfaces, as illustrated in Fig. 2, which appears in the Zarei et al. paper, in which they sketched the pie chart depending on 80+ relevant articles [30]. However, indoor experimental investigations of dust accumulation on PV generators have the potential to produce more reliable and accurate information [16]. In fact, many researchers widely used laboratory tests because of their controlled environment in which they can adjust, for example, the light intensity and the temperature, drawing more consistent results [36]. Furthermore, an indoor experiment's convenience manifests in fully controlling the dust sample concentration or deposition density [20], not to mention that the researchers can utilize different indoor experimental setups (e.g., test chambers), dust samples (e.g., ash, red soil, iron ore), laboratory tests (e.g., SEM, XRD, XRF), surface substrate materials (e.g., Acrylic plastic, low iron glass), PV device technologies (e.g., crystalline silicon, thin film), and numerous pieces of equipment to simulate the dust deposition mechanism, hence they can characterize its influence on the electrical performance, for instance Refs. [8,27].

The investigators' limited access to modern technologies or instruments urges many to be more innovative whenever a specific test or apparatus is missing to obtain dependable outcomes ultimately. Nevertheless, it is possible to detect a general pattern followed by all different indoor-based research. Therefore, future research needs to consider or be aware of the previous efforts that have already employed many advanced methodologies and utilized state-of-the-art or high-precision tools that helped to obtain comparable, rational, and interpretable results that describe different locations, dust deposition densities, dust materials, and particle sizes. Then, the gap that needs to be bridged here is between the sound practices with reasonable findings that already exist in the literature and the upcoming efforts that must benefit from these experiences or even rely on their techniques and outcomes in determining their research tracks. Accordingly, the methodology of the review article here will systematically deliver the relevant content depending on literature narration, information disaggregation by criteria, proper illustrations, and quality assessment of findings and methods. In the end, some recommendations regarding the best practices and future work directions will be provided, supporting this exhaustive attempt to overcome the mentioned void. In more concise wording, the foremost objective of this review study is to summarize the multiple and different experimental approaches utilized to simulate the dust deposition on top of PV structures inside laboratories, enabling the study of the accumulation effects on a range of PV characteristics to help eventually determine the best testing method according to the location and dust properties. Thus, the expected novelty of this work is to provide a viable pattern or model adapted from methodical approaches corresponding to targeted characterizations, which scientists will use to experimentally investigate the impact of dust soiling on the relevant PV characteristics.

Consequently, this article will contribute to the efforts aiming to standardize the tests of dust deposition on PV panels. Therefore, the rest of this article is organized as follows: Section 2 briefly describes the research methodology followed to direct the review, Section 3 presents how dust samples are chosen, and Section 4 outlines the physio-chemical properties, including morphological, mineralogical, and elemental descriptions. Section 5 lists the dust deposition surfaces and their dust removal and optical characterization practices, while Section 6 discusses the methods applied for the PV device's electrical and thermal characterization. Section 7 lists the experimental equipment and any dust deposition techniques, Section 8 suggests a systematic method according to the observations noticed throughout the article, and Section 9 and Section 10 conclude by providing a flowchart of the detected systematic methodology, a list of the vital pieces of equipment, and recommendations for future work.

2. Review methodology

Many methods in the literature have been used to simulate the dust-soiling process inside laboratories. For instance, Younis et al. manually scattered fine sand particles on a solar panel to simulate the physical phenomenon. For each 1g of plaster sand, the researchers wrote down the I_{sc} measurements to correlate dust amounts to the reduction in I_{sc} employing an empirical coefficient. Fig. 3 shows the panel inside a climate chamber after distributing around 59g of dust [37]. Following a similar approach, Güngör et al. distributed four samples of dust collected from industrial sites in Turkey using a manual sieving process while leaving the dust amount to be weighed after the finish of every dust material test as they were targeting the quantity that completely blocks the light from the panel surface or makes the output power equals to zero. This research revealed that the fine dust particles block more light than the grainy ones [38].

Noteworthy, there is no standard method for conducting dust-soiling simulation experiments, especially indoor ones, although observing a similarity between different experiment strategies is possible, encouraging many researchers to promote their work to be standardized [39]. Even some studies dictated a pattern for indoor experimentation of the dust-gathering effect [40], like the one demonstrated by the flowchart in Fig. 4, in which this research protocol was followed in several studies [41]. This sole situation motivated us, in this work, to script the broad lines that can highlight or provide a systematic methodology for conducting indoor experiments. For this reason, we reviewed over 70 papers published between 1993 and 2023 concerning the in-house dust deposition experiments on top of PV surfaces. Consequently, the

Table 1
Natural and artificial dust samples used in indoor experiments in the reviewed literature.

Reference	Location	Dust type	Dust material	Dust particle size (μm)
[51]	Tipaza, Algeria	Natural	• Soil	• 100–300
[43]	Aegean region, Turkey		• Coal	• >38 • 38–53 • 53–75 • 75–106 • 106–250 • 250–500
[52]	Al Batinah region, Oman		• Natural dust	• 2–75
[53]	Qatar and Namib desert		• Qatar natural dust • Namib desert sand	• 6–10 • 200–300
[54]	Al Batinah region, Oman		• Natural dust	• –
[55]	Inner Mongolia and Shandong, China		• Inner Mongolia's natural dust • Shandong natural dust	• 2.5–45 • 10–110
[56]	Belgium		• Aeolian dust	• 30
[57]	Sharjah, United Arab Emirates		• Natural dust	• 1.61–38.4
[58]	Kuwait		• Sand dust	• 6.44
[59]	India		• Sand	• 1.4–4.2
[60]	Oman		• Red soil • Carbonaceous fly ash • Sand • Calcium carbonate • Silica Gel	• –
[61]	Gdansk, Poland		• Natural dust	• 10–30
[62]	Gdansk, Poland		• Natural dust 1 • Natural dust 2 • Natural dust 3	• 200 and 450 • 230–360 • 220–330
[63]	Western Rajasthan, India		• Barmer dust • Bikaner dust • Jaisalmer dust • Jodhpur dust	• 125
[17]	Saudi Arabia		• Limestone	• 80
[40]	desert region, Iran		• Natural dust	• 1–30
[41]	Babuin, Indonesia, and Perth, Australia		• Babuin dust • Perth dust	• <4 (60 % of the particles) • <4 (65 % of the particles)
[64]	Qinghai, China		• Red soil	• 25
[65]	Eyjafjallajökull eruption in Iceland		• Tephra fine ash dust • Tephira coarse ash dust • Lapilli	• <60 • 200 - 600 • 14800
[66]	West Timor, Indonesia		• West Timor dust	• –
[67]	–	Artificial and natural	• Red clay • Silica	• 0.4–178 • 5 & 25 & 85
[48]	Tipaza, Algeria		• Cement • Soil • Sand • Salt • Gypsum • Ash	• 10 • 128.466 • 230.5 • 31.91 • 18.332 • 9.696
[44]	Baghdad, Iraq		• Ash • Sand • Red sand • Brown soil	–
[45]	Baghdad, Iraq		• Natural dust	40–45

Table 1 (*continued*)

Reference	Location	Dust type	Dust material	Dust particle size (μm)
[27]	Nigeria		• Calcium carbonate • Agricultural soil • Soot • Ash • Bird droppings • Carpet dust • Cement • Charcoal • Clay • Coarse sand • Laterite • Loam soil • Salt • Sandy soil • Stone dust • Wood dust	–
[68]	Sharjah, United Arab Emirates		• Artificial dust • Natural dust	• – • 0.37–0.68
[69]	Badarpur, India		• Badarpur sand 1 • Badarpur sand 2 • Fly ash • Rice husk • Chalk powder • Brick powder • Sand	• 50 • 50 • 50 • 10 • 10 • 10 • 10
[8]	Athens. Greece		• Red soil • Limestone • Carbonaceous fly ash	• ≤150 • ≤60 • ≤10
[70]	Henan Province and Guangzhou City, China		• A2 Test dust (ISO 12103-1), Powder Technology Inc, USA • Henan province dust • Guangzhou city • Construction site sand	• 0.3–20 • 100–4000 • 100–5000 • 100–3000
[71]	–		• –	–

Fig. 5. Powders of artificial and natural dust [27].

methodology used to conduct this study depends mainly on categorizing and narrating the relevant information, a step that necessarily requires initial content analysis so that this informative scientific text can be classified later. Also, each section of this article smoothly discusses and interprets its provided information. Moreover, in its narration, the review methodology utilizes the illustrative presentation technique through charts, figures, and tables, communicating different ideas and experimental approaches more effectively. In the end, the same methodology relies on the conclusion and recommendations for future work to clarify the most important observations, which inevitably reflect the

Table 2
Artificial dust samples used in indoor experiments in the reviewed literature.

Reference	Dust material	Dust particle size (μm)
[47]	• Cement • Plaster • Borax	–
[16]	• A2 Test dust (ISO 12103-1), Powder Technology Inc, USA	• 1–125
[72]	• –	–
[73–77]	• –	–
[78]	• –	–
[46]	• SiO_2 particles manufactured by Sigma Aldrich Ltd.	• 170 ± 20
[49]	• Calcium carbonate	• –
[79]	• Epoxy powder	• –
[80]	• Ash • Laterite • Stone dust • Sandy • Coal powder • Cement	• 12.22 • 343.56 • 1.56 • 6.54 • 8.69 • 5.82
[81]	• Red soil • Sand • White soil	• –
[82,83]	• Construction site dust	• –
[84]	• Absorbing mineral dust • Non-absorbing mineral dust	• –
[85]	• Dust • Sand	• 62–128
[37]	• Plaster soil	• –
[18]	• iron ore dust	• 600 - 850 • 300 - 600 • 150 - 300 • 75 - 150 • <75
[86]	–	–
[50]	• JSC Mars-1A simulant dust	• ≥1000 [87]
[88]	• Dried mud • Talcum powder	• –

Table 3
Electrical performance degradation in response to dust presence.

Reference	Deposition density (g/m^2)	Performance loss (%)	
		Output power	Conversion efficiency
[47]	–	–	>25.8
[16]	0–22	–	0–26
[52]	<1	–	0.05
[54]	5	1–12	–
[55]	0–10	–	7
[57]	1	1.7 (normalized power)	–
[61]	1 μm (layer thickness)	–	25.5
[62]	–	–	10
[63]	–	96.1	–
[17]	250	84	–
[40]	330	–	98.2
[27]	–	98	–
[68]	0–164.38	–	98.92
[8]	0.35	7.5	–
[88]	–	86	–

authors' analysis and perspectives, as these latter sections are a detailed explanation of this effort novelty rather than a monotonous summary of procedural steps.

3. Dust sampling

Classifying dust according to its emission source into artificial residues from manufacturing or vehicle movement and natural particulates from the surrounding environment is a well-established tradition in

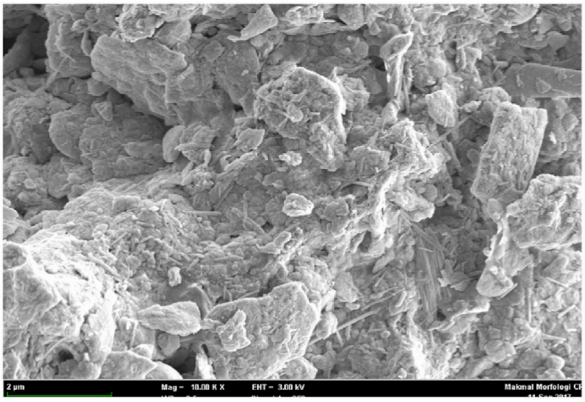

Fig. 6. SEM image of natural dust sample [68].

Table 4
SEM models used in the reviewed studies.

Reference	SEM model	Manufacturer	Secondary Electron Resolution
[61]	S–3400 N Variable Pressure	HITACHI	• 3.0 nm High Vacuum Mode • 4.0 nm Variable Pressure Mode [93]
[83]	S–3700 N		• 3 nm at 30 kV • 10 nm at 3 kV [94]
[64]	SU8000		• 1 nm at 15 kV • 1.3 nm at 1 kV [95]
[82]	SU8010		• 1 nm at 15 kV • 1.3 nm at 1 kV [96]
[73,77]	S-8820		5 nm [97]
[41]	JCM-6000 NeoScope Benchtop	JEOL	–
[40]	MIRA 3	TESCAN	• 1.2 nm at 30 kV • 2.3 nm at 3 kV [98]
[57]	VEGA3 XM Variable Pressure		• 2 nm at 30 kV • 2.5 nm at 30 kV [99]
[27]	Quanta 650 FEG	FEI	• 3.0 nm at 1 kV • 1.0 nm at 30 kV [100]
[63]	SEM-EDX	BRUKER	
[59]	Supra 40VP Field Emission	ZEISS	1 nm at 30 kV [101]

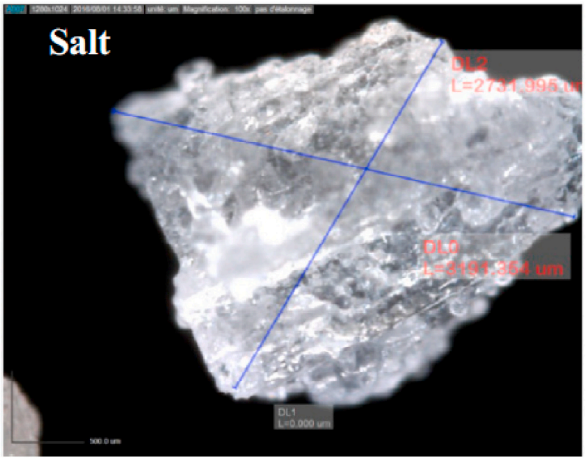

Fig. 7. A digital microscope image of a salt particle suspended on a glass coupon [48].

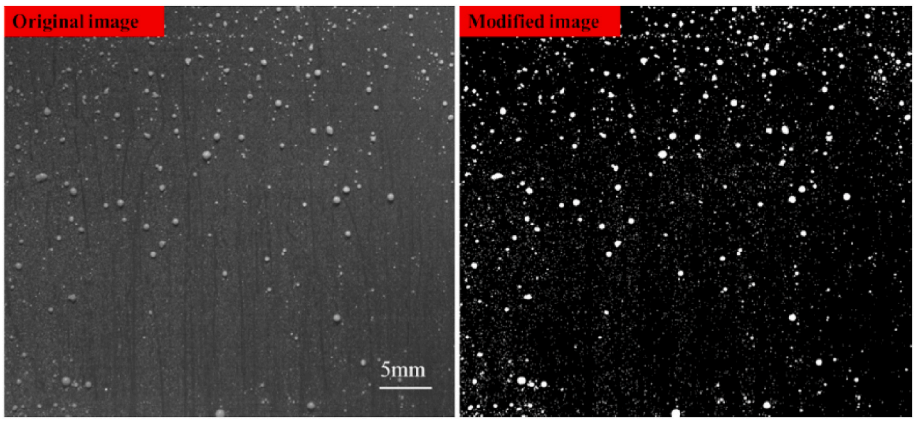

Fig. 8. CCD image before and after processing [67].

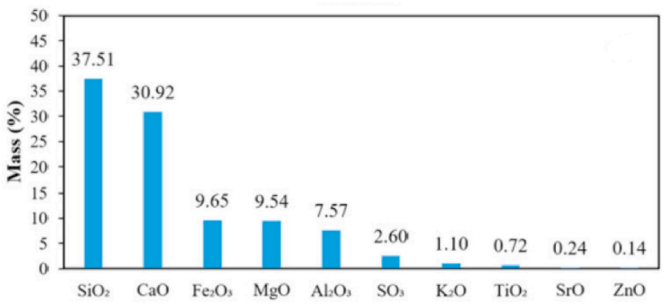

Fig. 9. XRF analysis of a natural dust sample [57].

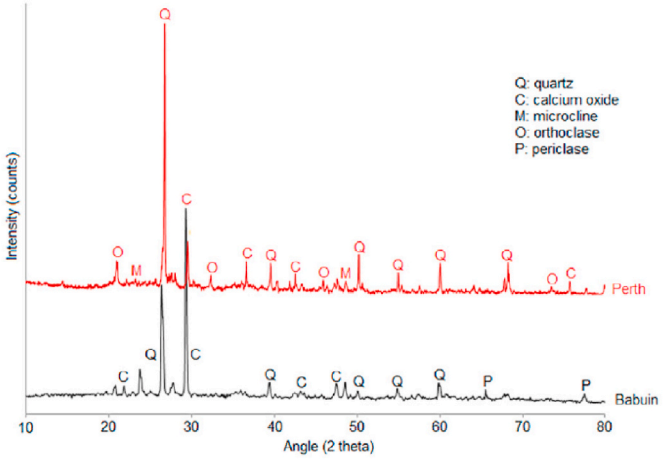

Fig. 10. XRD spectrum for natural dust collected from Perth and Babuin cities [41].

relevant studies [30]. In the literature, there are frequent types of dust material that were widely used in related experimental work, which are ash, carbon, calcium carbonate ($CaCO_3$), cement, clay, mud, red soil, ISO 12103-1 A2 test dust, limestone, sand, sand soil, silica gel, talcum, fine and coarser mode of air born dust, and coal dust [16,27,42]. Speaking of indoor or laboratory-based experiments only, Adıgüzel et al. investigated the effect of coal dust on the performance of mono-crystalline silicon (mono-Si) and poly-Si modules utilizing different particle sizes. They quantified the impact in terms of loss percentage. Fig. 32 shows the sieving technique by which the various coal dust samples were prepared or separated size-wise [43]. Also, Chaichan and Kazem experimentally examined the effect of ash, sand, red sand, and brown soil on mono-Si, poly-Si, and a-Si PV panels, and they obtained typical results that indicate a decrease in the PV performance by a percentage varies according to the type and amount of accumulated dust [44]. Different research by Chaichan and Kazem analyzed the effect of natural dust joined composition compared with its constituents on PV performance. They selected agricultural soil, soot, and $CaCO_3$ as the most prominent components in dust makeup in Baghdad, the city of the study, and accordingly carried out their analysis [45]. Table 1 lists natural dust samples used in the reviewed studies and their corresponding locations.

On the artificial dust side, Beattie et al. depended on manufactured SiO_2 sand particles of size 170 ± 20 μm to simulate the dust gathering on top of a glass slide, eventually deriving an exponential function that describes the relationship between the dust deposition density and the performance decline [46]. Emphasizing more, Abass et al. used aerosol particles of common construction materials available in Iraq: cement, plaster, and borax [47]. Moreover, Abderrezek and Fathi explored the effect of cement, soil, sand, salt, Gypsum, and ash on the electrical and thermal performance of PV panels, depending on indoor and outdoor experiments [48]. A study that focused on the effect of $CaCO_3$, which Darwish et al. did, reached a significant impact of these material particles on the I_{sc} [49]. Additionally, Chanchangi et al. evaluated the influence of thirteen different artificial and natural dust samples on the PV performance, always based on indoor experiments. Fig. 5 displays the samples' powders prepared for testing [27]. Also, Sayyah et al. used the JSC Mars-1A simulant dust, with particle diameter ranging up to 1000 μm, but with the assistance of a sieving process, 88 μm particles were separated and deposited on top of the targeted surface [50]. Table 2 provides an inventory of artificial dust samples used in the research reviewed within this article. It can be observed from the studies reviewed here that for the dust of natural origin, the more opaque the color of the dust, the greater the loss of performance, evidenced by Adiguzel et al. results, who obtained 62 % losses in power produced from poly-Si module covered by coal dust [43], at the same time Chichan et al. work revealed that red soil caused the most significant losses among different tested dust materials [44]. This preliminary conclusion makes sense, given that increasing color intensity means a more considerable decrease in passing light and vice versa.

4. Dust physio-chemical characterization

It has been identified by the researchers that dust has three fundamental characteristics; because of them, a decline in the PV performance occurs when it sets down on top of the module or any relevant assembly, which are the dust's chemical composition, particle size (or morphology or physical structure), and deposition density [89,90]. Of course, dust deposition density is the most influential factor that controls the degree of degradation [20]. Table 3 lists the percentage degradation in the

Table 5
Summary of mineralogical characterization executed in reviewed studies.

Reference	X-ray technology		Chemical composition	
	XRD	XRF	Component	Main contributor (weight %)
[55]	✓	✓	• $Na(AlSi_3O_8)$ • $KAl_2((Si_3Al)O_{10}(OH)_2)$ • SiO_2 • $Ca_5(SiO_4)_2(OH)_2$ • $Fe_3((FeSi)O_4(OH)_5)$ • $Ca(SiO_3)$ • NaCl • ZnO	• $Na(AlSi_3O_8)$
[52]	✓	✓	• Al_2O_3 • MgO • SiO_3 • SiO_2 • CaO • K_2O • Cr_2O_3 • TiO_2 • Fe_2O_3 • MnO_2 • SrO • NiO • P_2O_3 • Cl	• SiO_2 (55.79 %) • CaO (30 %)
[68]	✓	✓	• SiO_2 • CaO • Al_2O_3 • Fe_2O_3 • K_2O • MgO • TiO_2 • SiO_3 • Cr_2O_3 • MnO_2 • SrO • NiO	• SiO_2 (45.53 %) • CaO (24.62 %) • Al_2O_3 (10.83 %) • Fe_2O_3 (10.46 %)
[57]	×	✓	–	• SiO_2 (37.51 %) • CaO (30.92 %) • Fe_2O_3 (9.65 %)
[82]	×	✓	• SiO_2 • Al_2O_3 • Fe_2O_3 • MgO • CaO • Na_2O • K_2O • TiO_2 • BaO • P_2O_5	• SiO_2 (80.54 %) • Al_2O_3 (7.97 %) • Fe_2O_3 (1.49 %)
[83]	×	✓	• SiO_2 • CaO • Fe_2O_3 • Na_2O • K_2O • Al_2O_3 • SO_3 • P_2O_5 • MgO • Other	• SiO_2 (77.63 %) • CaO (3.44 %) • Fe_2O_3 (2 %)
[67]	×	✓	• SiO_2 • Al_2O_3 • K_2O • Na_2O • Fe_2O_3 • CaO • MgO	• SiO_2 (73.94 %) • Al_2O_3 (16.42 %) • K_2O (3.01 %)
[41]	✓	×	–	• SiO_2 • CaO
[63]	✓	×	• SiO_2 • $AlPO_4$ • $CaAl_2Si_2O_8$ • $CaCO_3$	• SiO_2 (38 %) • $AlPO_4$ (26 %)

Table 5 (*continued*)

Reference	X-ray technology		Chemical composition	
	XRD	XRF	Component	Main contributor (weight %)
[40]	×	✓	• SiO_2 • CaO • Al_2O_3 • Fe_2O_3 • MgO • K_2O • Na2O • TiO_2 • P_2O_5 • MnO	• SiO_2 (44 %) • CaO (14.28 %) • Al_2O_3 (9.95 %)
[61]	–	–	• SiO_2 • Al_2O_3 • MgO • Fe_2O_3	• SiO_2

output power and conversion efficiency related to dust deposition density and material. As a quick reminder, the conversion efficiency of a solar cell is the ratio of the output electrical energy to the incident light energy [91]. Therefore, the numbers in the earlier table refer to the losses in this efficiency, although they are calculated in percentages. It can be briefly discussed here that these figures prove the strong relationship between the deposition density and performance losses of the PV devices, as densities greater than 100 g/m^2 resulted in more than 80 % losses. Hence, studies with a transparent research methodology depend on the physio-chemical characterization of dust particles using well-established techniques to deliver more solid and scientific diagnostics of the dust interactions with PV surfaces or electrical performance.

4.1. Morphological characterization

Scanning electron microscope (SEM) imaging is most frequently used to determine the morphology of dust particles, as the research proves that the shape and size of the dust particle influence the PV performance degradation [17]. In other words, the main characteristics that could be extracted from the SEM image, using software like ImageJ, that sufficiently describe the physical nature of the dust are the particle mean diameter (i.e., size) and its standard deviation [17]. For the indoor evaluation of PV devices under dust-soiling conditions, many researchers started their work by analyzing the SEM images they obtained for their natural or artificial dust samples to determine their appropriate particle sizes, usually in micrometers [27,41,53–55,57,59,61,63,65,68,69,80,82]. Darwish et al. examined a selection of natural dust samples using SEM imaging and noticed non-homogenous shapes with a diameter range between 0.37 and 0.68 μm. Fig. 6 shows the obtained SEM scan [68]. Also, Hussain et al. analyzed the SEM images obtained for different artificial and natural dust samples and concluded that the finer the particles, the greater the PV power loss, with rice husk powder causing the most significant decrease [69].

Moreover, Huang et al. used the SEM to discover that the dust particles under study were irregular in shape and size [82]. Emphasizing the irregularity, Hachicha et al. depended on SEM imaging to disclose that dust particles under investigation had an uneven size distribution, ranging between 1.61 and 38.4 μm [57]. Table 4 lists the SEM models used in the relevant experiments to inspect dust particle topography. It is worth mentioning that some researchers relied on digital [48,78,85], electron [45], optical [17,46], and regular [92] microscopes to conduct the same morphology and particle size analysis. Fig. 7 demonstrates a digital microscope image of a salt particle deposited on a glass slide [48]. Yuan et al. depended on a different approach, in which they took images with a charge-coupled device (CCD) camera and then processed the images to prepare them for ImageJ software, which enables

Table 6
Summary of elemental characterization executed in reviewed studies.

Reference	Chemical composition	
	Element	Main contributor (weight%)
[82]	• Si • O • Al • P • Ca • Na • Mg • S	• Si (48.86 %) • O (46.18 %)
[57]	• O • C • Ca • Si • Mg • Fe • Al • Cu • Na • K • S • Cl	• O (46.1 %) • C (20.3 %)
[83]	• O • Si • C • Ca • Al • Na • Fe • K • Mg • P • S	• Si (40.92 %) • O (45.06 %)
[41]	• O • Si • Ca • Al • Fe • K	• O (34 %) • Si (29.14 %)
	• Ca • O • Fe • Si • Al • Mg • K	• Ca (32.42 %) • O (24.59 %)
[53]	• Si • Al • K • Fe • Ca • Mg • Others	• Si (76 %) • Al (9 %)
	• Ca • Si • Fe • Mg • Al • K • Others	• Ca (64 %) • O (14 %)
[63]	• O • Si • Al • C • Ca • Fe • K • Mg • Na	• O (62.25 %) • Si (19.61 %)
[40]	• Si • O • Al • C • Ca • Mg	• Si • O
[61]	• K • Fe • Si • Al • Mg • Fe • K • Ca • P • S	• Si

obtaining the morphological characteristics of dust particles. Fig. 8 shows a CCD image before and after processing, made ready for use by the software [67]. It is necessary to mention here that a common finding in most of the research that considers the morphological characterization in its analysis is that the smaller the dust particle, the more the performance loss and vice versa.

4.2. Mineralogical characterization

Dust chemical composition supports the existence of adhesion forces between the particles and the relevant surface. The availability of such information helps pick a suitable cleaning method, determine dust's optical properties, and sort out its source [40]. X-ray diffraction (XRD) and X-ray fluorescence (XRF) are the most used techniques by researchers in the reviewed literature to conduct mineralogical analysis or study the chemical composition of the natural dust accumulating on PV devices. For these methods, Bruker D8 Advance and Horiba XGT-7200 models are examples of popular XRD and XRF instruments used in relevant dust-soiling studies, respectively [52,68]. Of course, there are incidences where researchers used the same devices to analyze artificial dust, like the works of Huang et al. [82] and Quan and Zhang [83], in which they deposited particulates obtained from construction sites on top of PV modules. Still, they traced Silicon dioxide (SiO_2), which was dominating, similar to natural dust composition. Fig. 9 represents the XRF results of natural dust analysis [57], while Fig. 10 shows the XRD spectrum graph, a different format of the results. Meanwhile, Table 5 summarizes the mineralogical characterization results of dust samples mentioned in the relevant literature, listing them in descending order according to the weight percentage of each component. To sum up, employing the mineralogical analysis tools, mainly XRF and XRD devices, SiO_2 was the dominant natural dust constituent available in abundance in every sample.

4.3. Elemental characterization

Energy-dispersive X-ray spectroscopy (EDS or EDX) is another widely spread X-ray technique for the elemental characterization of natural and artificial dust samples used in the relevant research. The benefit of this method is that it can determine the chemical composition of the sample element-wise. An example of an EDS machine model is the Oxford Instruments X-Max 50 EDS detector [57]. Huang et al. and Quan and Zhang analyzed artificial dust samples collected from construction sites to know their constituent elements depending on the same EDS technology [82,83]. Similarly, Chanchangi et al. relied on the EDX to determine the components for a spectrum of natural and artificial pollutants listed in Tables 2 and in which they unveiled the presence of Fairchildite, Manganese, Amphibole, Richterite, Silica, Xenotime, Olivine, Monticellite, Calcite, Hatrurite, Brownmillerite, Ankerite, Charcoal, Beryl, and many others [27]. Table 6 summarizes the elemental composition of some dust samples, delivering them in descending order according to the weight percentage. A noticeable observation is that the EDS detector, responsible for the elemental

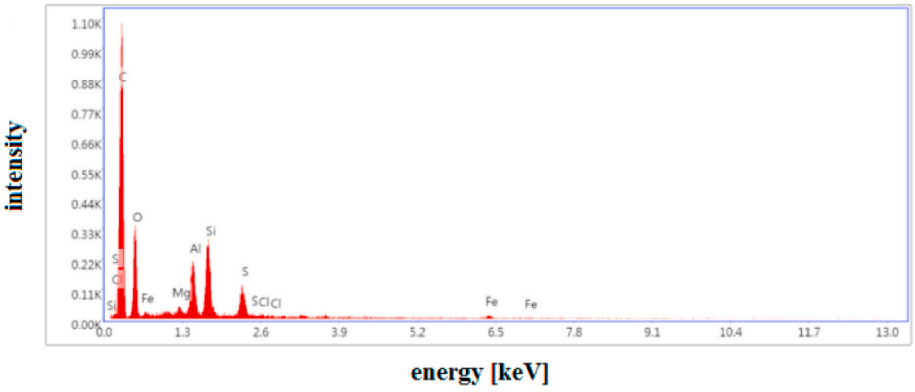

Fig. 11. EDS graph for natural dust sample [62].

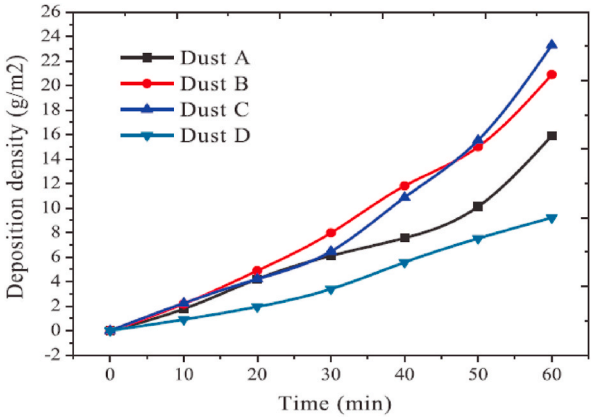

Fig. 12. Dust deposition density rate on a coated surface with different dust materials: A) Artificial dust (A2 Test, ISO 12103-1) B) Henan province dust C) Guangzhou city dust D) Construction site sand [70].

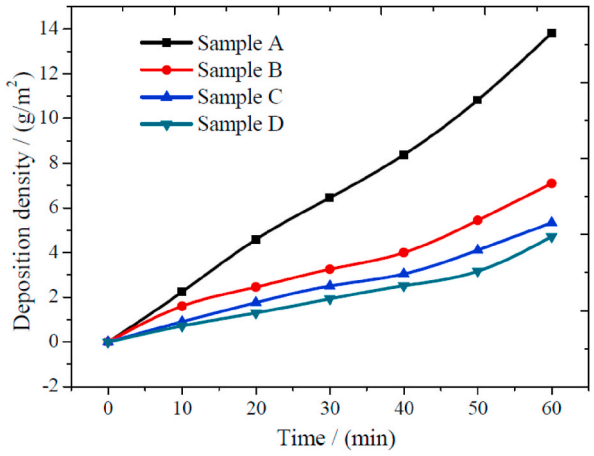

Fig. 13. Dust deposition density rate with different coatings: A) Without coating B) Hydrophobic silica solution C) Ethanol solution with SiO_2 nanoparticles D) Silica solution with SiO_2 nanoparticles [77].

analysis, presented oxygen (O) and silicon (Si) interchangeably as the most available elements in most samples (see Fig. 11)

5. Deposition surface characterization

In the literature, the researchers mainly depended on PV modules [17,18,37,63–65,71,85,86,88,102], glass coupons [48,67,70,73,76,77,

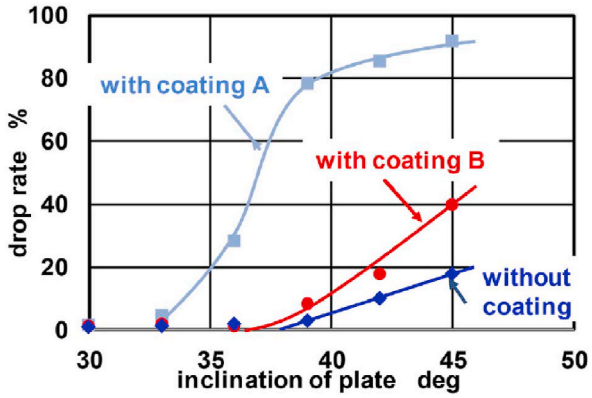

Fig. 14. Effect of self-cleaning coating on the adhesion forces of glass plate [53].

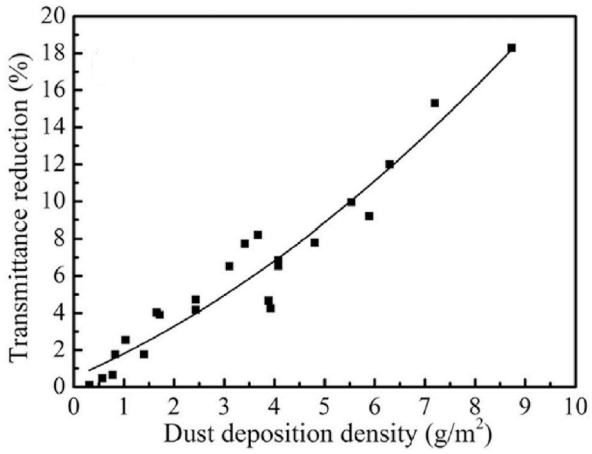

Fig. 15. Transmittance reduction Vs. Dust deposition density for the transparent hydrophobic coated glass slide [83].

103], both [41,66], or acrylic board [104] to represent the deposition surfaces needed for their indoor experiments. Accordingly, the characteristics that change with surface type are the surface adhesion or dust-removal and the optical properties.

5.1. Dust removal characterization

In this subsection, studies on characterizing dust removal properties of the deposition surface based on laboratory tests were targeted. Many

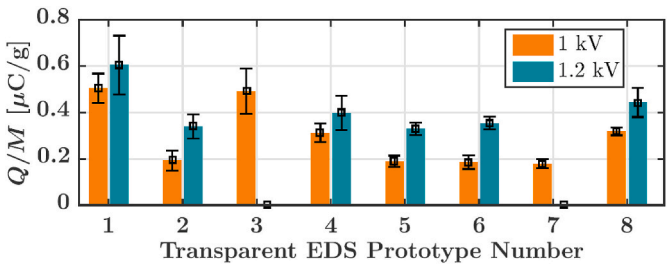

Fig. 16. Q/M measurements for eight transparent EDSs at different applied voltages [50].

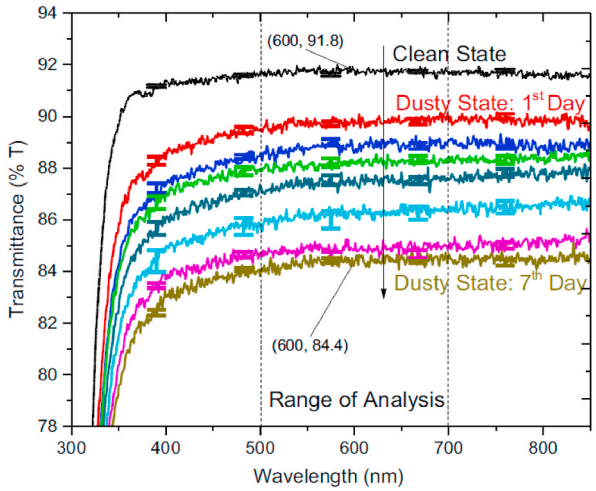

Fig. 17. Reduction in low-iron glass transmittance due to dust accumulation [108].

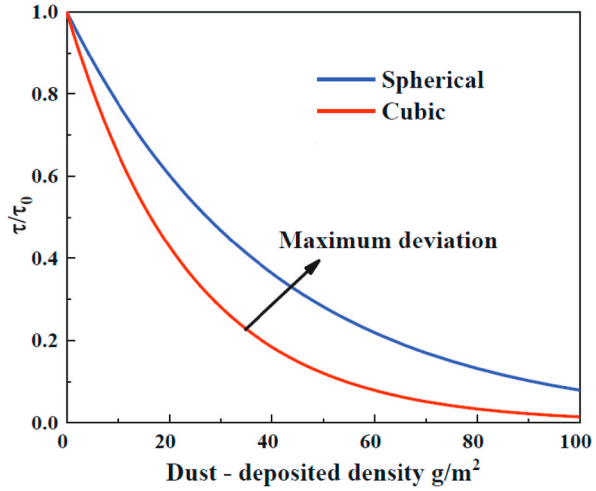

Fig. 18. Effect of dust particle morphology on the glass transmittance at a variable deposition density [104].

indoor experiments were designed to examine and evaluate the reduction of the accumulated dust on a coated glass cover or PV surface. The pivotal characteristics of these deposited transparent coatings hover around, accelerating the sliding of dust particles out of the inclined PV façades. These dust removal techniques can be categorized into passive and active [105]. It is the customary practice among the reviewed literature here to have a variable tilt angle along with an airstream within an enclosed test rig to simulate the dust agglomeration on the deposition surface and then facilitate studying the anti-soiling properties of a specific coat [64,70,73,76,77,82,83]. Fig. 23 shows a typical test chamber with a fan and an adjustable stand or tray [70,73,77]. Starting with the passive removal group, self-cleaning coatings that ease the dropping of dust particles are the most common method. Lu et al. investigated the anti-soiling capacity of super-hydrophobic coatings employing natural and artificial dust. They found that construction site sand was repelled the most from the coated surface, represented by deposition density equivalent to 36.77 % of the uncoated PV glass sheet density. Fig. 12 displays the interaction between the coated glass and dust materials utilizing the dust deposition density rate. For the tests conducted in this study, the researchers employed the same setting illustrated by the earlier figure (i.e., Fig. 23) [70]. Zhang et al. explored the reduction in dust gathering on a PV module enveloped with a transparent super-hydrophobic coating utilizing indoor tests, which showed significantly few amounts left due to low surface adhesion forces at large tilt angles, quantified by deposition density of 11.2 % of the uncoated glass plate density for tilt angle 60°. Also, the spectral transmittance and conversion efficiency were higher than the uncoated glass's. Considering the PV technology, the super coating performed better with poly-Si modules [52], not forgetting that artificial or natural dust has the same effect. As accustomed, the research team in this study used a test setting similar to the one illustrated in the earliest figure [52]. Pan et al. utilized numerous self-cleaning coatings (i.e., hydrophobic silica solution, ethanol solution with SiO_2 nano-particles, silica solution with SiO_2 nanoparticles), the standard test chamber of the earliest figure, and 30° inclined glass samples to find that the super-hydrophobic silica coating with micro-nano SiO_2 structures has the best dust removal characteristics resulting in 36.1 % deposition density of the uncoated glass piece. Fig. 13 illustrates the coatings' effects on the dust deposition density rate [77]. Lu et al., who depended on indoor wind tunnel tests, studied the effects of tilt angle, wind speed, and wind direction on the dust removal quality of the super-hydrophobic film. The wind tunnel was well-equipped with features that enabled it to control the mentioned three parameters. Then, through the experiments, the researchers noticed that the self-cleaning coating had 94.43 % dust prevention efficiency at a 75° tilt angle, 25 % at low wind speeds, and 65.85 % facing the wind direction. Fig. 27 shows the wind tunnel platform used in this study [76]. Wang et al. tested PV modules coated with silicon-based and fluorine-based super-hydrophobic films and covered with dust to find that these coatings effectively removed the dust with extra advantage to the fluorine film, as the drop in the maximum produced power was (0.92 ± 0.08)%, while for the silicon film was (1.36 ± 0.07)% [64]. Kawamoto and Guo integrated two-phase high-voltage electrodes and anti-soiling coating within an inclined glass plate to develop a cleaning system. For that, the researchers tested the dust removal characteristics of the hydrophobic anti-soiling coatings, namely A and B, which were silicon-based and fluorine-based, by scattering a uniform layer of natural dust and measuring its drop rate, which is the weight of the falling dust amount divided by the initial accumulating weight. The team revealed that the investigated coatings reduced the adhesion forces by a great deal, as shown in Fig. 14 [53].Yuan et al. controlled the temperature and humidity of a unique indoor setup, illustrated in Fig. 28, to investigate the super-hydrophobic layer's dust removal effectiveness if condensation is present. The researchers found that 95 % of the dust particles were carried away within 90 min when the air temperature was 26 ± 0.5 °C and the humidity was 60 ± 5 % [67]. Quan and Zhang executed four experiments regarding the dust interaction with glass slides coated by a cost-effective layer: dust collision, employing the setup in the earliest figure, and dust removal experiments. For dust deposition and impinging investigation, a high-speed camera was used to capture the process, and the decrease in the transmittance was used to quantify the accumulating amounts. Fig. 15 shows the transmittance reduction against the dust deposition density for the glass slides coated by silica solution with SiO_2 nanoparticles. On the dust removal experimentation side, the researchers concluded that the low energy and rough coating surface lessened the

Table 7
Summary of instruments used in optical characterization by the reviewed literature.

Reference	Equipment	Model	Manufacturer	Resolution	Measured parameter
[78]	UV-VIS Spectrophotometer	UV-2600	Shimadzu	0.1 nm [109]	Transmittance
[73,77,83]	UV spectrometer	U-3010	–	–	
[64,104]	UV-VIS-NIR Spectrophotometer	UV-3600	Shimadzu	0.1 nm [110]	
[108]	UV–VIS spectrophotometer	Thermo Scientific Evolution 600	–	–	
[27]	UV/VIS/NIR Spectrophotometer	Lambda 1050	PerkinElmer	<0.05 nm [111]	
[58]	spectrophotometer	KONTRON UVIKON 860	–	–	
[41,66]	HP spectrophotometer	–	–	–	
[92]	Spectrophotometer	–	–	–	
[70]	UV spectrometer	–	–	–	
[55]	• Optical fiber spectrometer • reflectance and transmittance integrating sphere	• USB2000 fiber optic spectrometer • INT-38R reflectance integrating sphere • INT-36T-2 transmittance integrating sphere	• Ocean Insight	• 0.3–10 nm [112]	Reflectance and transmittance
[84]	UV/VIS/NIR spectrophotometer with integrating sphere	Lambda 1050	PerkinElmer	<0.05 nm [111]	
[58]	Spectrophotometer with integrating sphere	Beckman ACTA MIV	–	–	Reflectance
[48]	spectrophotometer	CL 500A	Konica Minolta	–	• Transmission coefficient • light spectrum

adhesion forces regardless of the degree of hydrophobicity [83]. Here, we must look at a point of great importance: the effect of the super-hydrophobic coatings on the optical properties of the glass cover or the deposition surface. It must be mentioned that the principle of these coatings depends on the surface roughness, a characteristic that is difficult to coexist with the optical transmittance if the optical performance of that surface needs to be maintained. Therefore, optimizing the surface roughness while fabricating these transparent self-cleaning coatings is a requisite [106].

On the second end of the passive dust removal techniques spectrum, some studies solely relied on the mechanical discharge of the unwanted dust by using indoor setups with adjustable features that control the tilt angle and the airstream like what we have already unveiled in the earliest figure [58].

Regarding the active or automatic dust removal process, the transparent electrodynamic screen (EDS) technology, which charges the dust particles with electrostatic force to facilitate their direct removal by the traveling electric field, is the most popular in this group but still immature enough to be deployed on a large scale [107]. A second shortcoming is that the electrostatic-based see-through films require a dry atmosphere to function, making them, at the moment, only suitable for semi-arid and desert climates [105]. Guo et al. investigated the dust removal efficiency of an EDS taped to a thin glass plate to find that the efficiency relevant to the dust deposited by the aerosol deposition system, illustrated in Fig. 42, is lower than that of the dust deposited by the sieve deposition mechanism [107]. Sayyah et al., in their work, aimed to test and measure the dust removal properties of different EDS prototypes employing the dust charge-to-mass ratio (Q/M), as illustrated in Fig. 16. The researchers used a humidity-controlled test chamber fixed in their laboratory, in which a vibratory sieve was installed to scatter the dust particles on top of the EDS samples [50]. It should be mentioned here that there are many other methods for removing dust from PV surfaces, whether active or passive, such as hydrophilic coatings and ultrasonic self-cleaning [21]. However, some techniques are not included in this comprehensive review because no significant analysis results were found in the relevant studies regarding the effect of these methods on the adhesion properties of the solar panel surface.

5.2. Optical characterization

For the optical characterization, the emphasis is always on describing the transmittance and reflectance of surface material facing the dust presence, as dust can reduce the transmittance by more than 50 % [84]. This material is commonly acrylic plastic [7,104] or low iron glass [46,48,58,66,103,108], bearing in mind that Chanchangi et al. concluded that acrylic plastic gathers more dust than glass [27]. Regarding the equipment used, most reviewed studies relied on different spectrophotometer technologies and models to measure the surface material's optical qualities after dust accumulation [64,70,73,77,83,92,104]. Al Shehri et al. used a UV–VIS spectrophotometer to discover a decline in the transmittance due to one-week exposure of the glass coupon to outdoor dust accumulation, as demonstrated in Fig. 17 [108]. Also, Piedra et al. employed a UV/VIS/NIR spectrophotometer with an integrating sphere to obtain a linear degradation of optical transmittance with deposited dust mass per unit area depending on glass slides for their indoor tests [84]. Interesting results obtained by Wu et al. using a UV spectrophotometer showed that cubic dust particles reduced the transmittance of the acrylic board more than spherical ones, all illustrated in Fig. 18 [104]. Table 7 lists the instruments widely used in the reviewed literature to measure the optical response of PV surfaces after applying dust layers.

6. PV module characterization

Solar PV generators are currently the most mature clean energy technology, considered a compelling power source in many countries. The PV cell performance has been continuously studied against environmental conditions to help the electricity-generating device operate at its maximum capacity [17]. The interest in PV effectiveness facing dust deposition has been going on since the forties of the last century [113]. Most of the related works focused on examining the impact of dust on the electrical and thermal characteristics of PV panels [18,60,74,75,80,86,114–116], which are, in their turn, mostly either mono-Si, poly-Si, or a-Si technologies [43,44,54,66,68,117]. Table 8 inventories the PV technologies mentioned in the reviewed literature concerned with laboratory experiments of the dust deposition effect.

6.1. Electrical characterization

It is well-documented that PV performance deteriorates proportionally with the dust deposition density [27], regardless of the particle size or shape [43], while dust agglomeration on PV panels significantly affects the I_{sc}, whether indoors or outdoors [20]. In the relevant literature, many researchers focused on measuring the electrical characteristics of PV panels in response to dust soiling. Of course, they depended on indoor experiments that created controlled environments using the appropriate equipment. Abass et al. studied the effect of artificial dust on the efficiency and output power of PV panels, utilizing a test bench

Table 8
Specifications of PV modules used in the indoor experiments in the reviewed studies.

Reference	PV technology	Module dimensions (cm x cm)	Module capacity (W_p)
[68]	Mono-Si	133.5 × 5.47	100
[48]		65.6 × 30.6	20
[102]		25 × 18.5	5
[80]		44.5 × 54	30
[65]		67.5 × 34.5	30
		38.3 × 29.9	10
[88]		63.5 × 53.5	50
[61]		–	70
		–	75
		–	100
[37]		–	50
[75]		13.5 × 13.5	–
[74]		15.6 × 15.6	–
[118]		51 × 53.5	–
[40]		6 × 4	0.75
[55]		12.5 × 12.5	–
[71]		100.4 × 44.8	50
[117]	Poly-Si	67.5 × 45.8	37
[60]		44 × 28.2	10
[49]		99.8 × 67.6	100
[18]		–	20
[86]		–	20
[81]		41.5 × 26.8	10
[57]		26.5 × 16	5
[69]		–	60
[56]		10 × 10	–
[79]	a-Si	• 28 × 70 • 15 × 5.5 • 1.25 × 1.65	–
[43]	• Mono-Si • Poly-Si	• 66 × 53 • 66 × 60	• 50 • 50
[54]		• 101 × 66 • 101.2 × 66	• 100 • 100
[62]		• 121 × 52.6 • 68 × 35.3 & 119.5 × 54.1	• 75 • 30 & 85
[44]	• Mono-Si • Poly-Si • a-Si	• 44 × 28.2 • 44 × 28.2 • –	• 10 • 10 • 10
[16]		• 12.5 × 12.5 • 12.5 × 12.5 • 12.5 × 18	–
[66]		–	• 119.35 • 76 • 29.21
[41]		–	–
[72]		• 10.2 × 10.2 • 10.2 × 10.2 • 10.2 × 10.2	–

equipped with a fixed irradiance light source and a multimeter for current and voltage determination, concluding a performance loss of up to 25.8 % [47]. Also, Jiang et al. examined the natural dust accumulation effect on PV panels using a test chamber that contains a solar simulator, and for the electrical parameters, they used an I – V tracer to obtain the I – V and P – V curves [16]. Moreover, Chanchangi et al. investigated thirteen different dust samples to conclude that charcoal resulted in a 98 % loss of the I_{sc} depending on the built-in features of a solar simulator to take the measurements [27]. Chaichan and Kazem dispersed natural dust on top of a PV module within an indoor testing setup and evaluated the electrical response using a digital voltmeter to notice that current and voltage decline occurred, for the first time, at low dust deposition density [45]. It is essential to highlight the role of external resistance or load (variable or fixed) in measuring the electrical features of the PV module under the test in the absence of competent equipment (i.e., I – V curve tracer), as variable load helps obtain the I – V curve characteristics while the fixed load finds the current and voltage of the PV panel. For example, some researchers used voltage and current sensors connected to fixed and variable loads to quantify the degradation in the panel's performance due to dust presence [49,68]. Table 9 delivers a summary of the pieces of equipment needed to conduct the electrical appraisal of PV modules under dust-gathering conditions.

6.2. Thermal characterization

The PV module efficiency is strongly associated with the operating temperature [102]. The typical conclusion in many relevant studies is that the PV device's temperature rises because of the blocked heat dissipation caused by the dust cover at the top [33,131–134]. Consequently, many researchers were concerned about the thermal response of the dust-soiled PV panels based on indoor tests. In these studies, a heating source and a dark room or space were needed to create a temperature gradient while maintaining a controlled environment to assess the impact of dust deposition on the temperature of the PV module [74,75]. The investigators revealed that a higher temperature gradient between the PV surface and the surroundings lowers, to some extent, the dust deposition density due to the Thermophoresis, leading to relatively increased performance, prominently for temperature gradient less than 40C°, as illustrated in Fig. 19 [74,75]. It is briefly recalled here that Thermophoresis is the phenomenon that occurs when tiny particles in a temperature gradient travel from hot to cold regions [135]. Xu et al. focused on the thermal characterization of the glass cover of the PV module by testing a glass slide within an indoor setup similar to the one always referred to as the earliest figure (i.e., Fig. 23) to evaluate its response following temperature rise and dust deposition to find that the upper temperature of the plate increased by 64.7 % and the lower by 33.3 %, compared to the clean glass sheet, resulting in 1.106 °C difference between ambient and dusty glass temperatures. Fig. 20 shows more detailed results, emphasizing the upper and lower surface temperatures [103]. Tripathi et al. obtained a 12.32 % increase in the surface temperature of the dusty PV panel compared to the clean one. Fig. 21 illustrates the significant findings regarding the surface temperature of the PV module covered by different dust amounts [86]. Table 10 lists the instruments used for the thermal assessment and their corresponding measured parameters.

7. Experimental equipment and techniques

7.1. Indoor setup

In this section, the standard types of equipment present in every indoor testing setup were addressed, summarized later in Table 16 in the conclusion section. It is vital to maintain a controlled indoor environment by manipulating the room temperature and humidity, primarily to exclude any undesirable effects of these factors on the dust deposition process or to study the effect of each factor in isolation from the rest. Many studies resorted to air-conditioning units to achieve this goal by controlling in-house conditions [16,43,52,67,82,115]. For instance, Huang et al. used an air-conditioning unit to keep a relative humidity between 40 and 50 % [82]. Also, Adıgüzel et al. utilized the same unit to set the temperature to 25 C° [43]. In addition, Sayyah et al. employed a humidity-control system with a sensor, humidifier, and dehumidifier to adjust the moisture content inside the test chamber [50]. Basically and effectively, Katoch et al. used a typical fan to cool down the PV cell exposed to the solar simulator's light [59]. Fig. 22 illustrates an indoor setup schematic design with the necessary test equipment [55].

7.1.1. Test chamber

The majority of reviewed studies endorsed the environmentally controlled enclosure approach for simulating the natural dust deposition on PV panels [16,50,55,58,61,64,70,72–75,77,80,82–84,103,118], in which a test chamber is equipped with a generator or launcher that supplies the rig with the dust that will settle on the assigned deposition surface assisted by artificial airflow or make do with the natural

Table 9
Summary of electrical characterization instruments mentioned in the reviewed literature.

Reference	Equipment	Manufacturer	Model	Accuracy	Measured parameters
[47]	• Multimeter • Electric load	–	–	–	Current and voltage
[54]	• Digital voltmeter • Digital ammeter	–	–	–	
[69]	• Multimeter • Rheostat load	MASTECH	M3900	0.5 % [119]	
[68]	• Variable thermal resistance • Current and voltage sensors	–	–	–	
[49]	• Constant resistance • Current and voltage sensors	–	–	–	
[27]	Continuous solar simulator	Wacom	–	–	
[45]	• Digital voltmeter	HAILANGNIAO	–	–	
[61]	• variable resistance • Universal digital multimeter	–	–	–	
[85]	• Digital multimeter	–	–	–	
[81]	• Digital multimeter	–	–	–	
[65]	• Aluminium-housed fixed resistor • Ammeter • Voltmeter	–	–	–	
[71]	• Analog multimeter	Sanwa	YX360TRF	±3–5 % [120]	
[17]	• Digital multivoltmeter	–	–	–	
[88]	• Digital multimeter	Proskit	MT-1210	1 % [121]	
[18,86]	• Ammeter • Voltmeter	–	–	–	
[16]	• I – V curve tracer	EKO PROVA	MP-160 –	±0.5 [122] –	I – V curve characteristics
[40]		Ivium	IviumStat.h standard	±5A, ±10V [123]	
[117]		MECO	9009 Solar Module Analyzer	±1 % [124]	
[80,114]		PROVA	PROVA 1011	±1 % [125]	
[63]		–	PROVA 210	±1 % [125]	
[48]		–	–	–	
[59]	• data logger	–	–	–	
[62]	• Solar module measurements	Gunt Hamburg	ET 250 [126]	–	
[41,66]	• Solar simulator	Eternalsunspire	SPI-SUN 5600SLP BLUE	Class A [127]	
[68]	• DC electronic load • Current and voltage sensors	Circuit Specialists	Array 3711A	0.2 % [128]	
[49]	• Electric variable resistance • Current and voltage sensors	–	–	–	
[57]	• Source measure unit	Tektronix	Keithley SMU	±0.015 %	
[56]	• Oscilloscope • Variable resistor	Hameg	HM203-5	–	
[55]	• Source measure unit	Tektronix	Keithley2460	±0.015–0.025 % [129]	
[64]	• I–V curve tracer	PROVA	Prova 200A	±1 % [125]	I – V and P – V curve characteristics
[102]	• Ammeter • Voltmeter • Variable load Rheostat	–	–	–	
[55]	• Source measure unit	Tektronix	Keithley 2460	±0.015–0.025 % [129]	maximum current, maximum voltage, maximum power, open-circuit voltage, and short-circuit current
[60]	• Digital multimeter	–	–	–	Voltage and power
[79]	• A custom-made instrument with static Faraday Cups on an FR4-PCB	–	–	–	voltage
[116]	• Multimeter • Variable resistor	–	–	–	Short-circuit current, open-circuit voltage, I – V curve characteristics
[37]	• Digital Multimeter	Proskit	MT-1280	0.5–3 % [130]	Short-circuit current

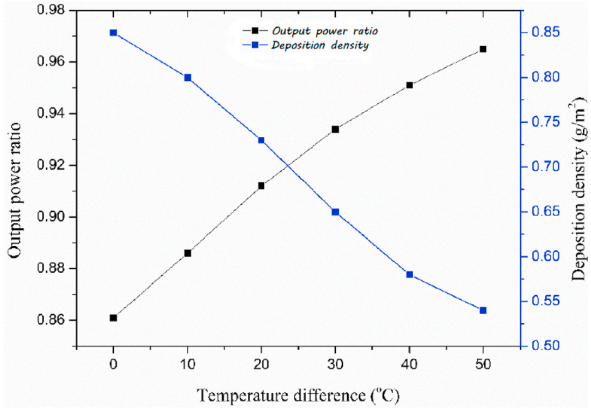

Fig. 19. Output power ratio between clean and dusty module Vs. Difference between ambient and PV module surface temperature Vs. Dust deposition density [75].

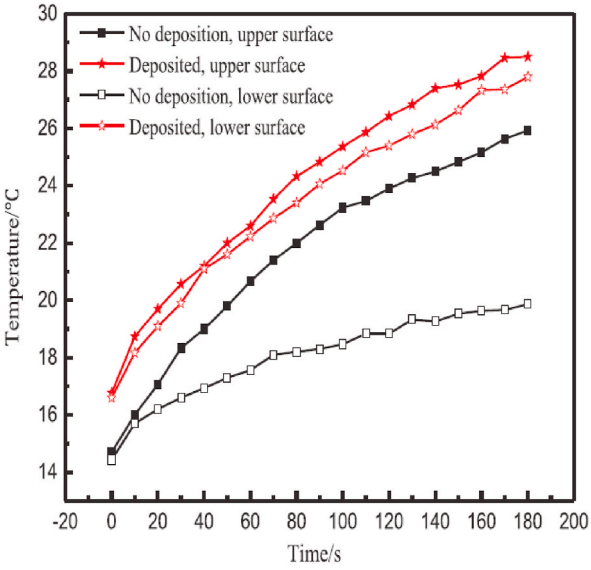

Fig. 20. Dust effect on glass plate temperature resulting from indoor experiments [103].

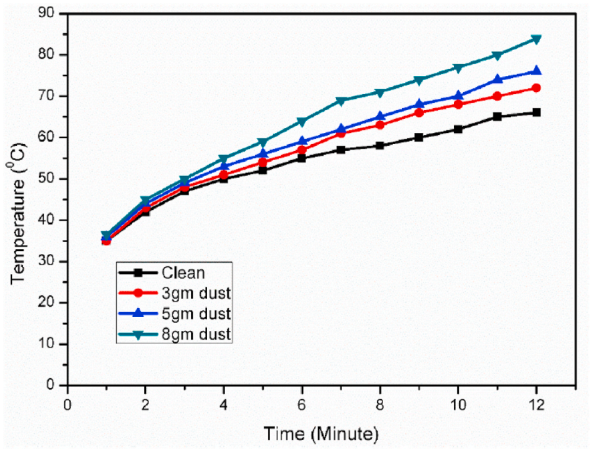

Fig. 21. Dust effect on PV module surface temperature resulting from indoor experiments [86].

Table 10
Summary of equipment used for thermal characterization in the reviewed literature.

Reference	Equipment	Measured parameter
[118]	• HT-9815 thermocouple • Thermometer	Surface temperature
[62]	• Pyrometer	
[85]	• Digital thermometer	
[103]	• Infrared thermometer	
[86]	• Pyrometer	
[17]	• Copper-constantan thermocouple	
[55]	• Thermocouple • Temperature controller	Backside temperature
[115]	• K-type thermocouple	
[59]	• PT100 Thermocouple	
[45]	• Temperature sensor	
[117]	• Infrared thermometer	
[37]	• Class B PT100 temperature sensors	
[68]	• Temperature sensor	Front frame and backside temperatures
[49]	• IC temperature sensors	
[16]	• T-type thermocouple	Module temperature
[54]	• Digital thermometer	
[81]	• Temperature sensor	
[114]	• Temperature sensor	
[60]	• AR922 Infrared Thermometer	
[74,75]	• Heating plate • Temperature sensor • Dark environment	Temperature gradient
[116]	• Platinum resistance thermometer	Cell temperature

airstream. Fig. 23 displays a typical test chamber deployed in many relevant studies [70,73,77]. An example of a standard dust generation unit is the RBG 1000, manufactured by PALAS GmbH [16,74,75], shown in Fig. 24 [20]. The chamber developed by the National Solar Energy Institute (CEA- INES) is an excellent example of an environmentally controlled enclosure for dust-soiling experiments, as presented in Fig. 25 [78]. In some designs of the test chambers, researchers used different auxiliary equipment like a blower [55], a stirrer [82], or a particle counter that helps detect dust concentration and distribution [73]. Also, a necessary structure inside this test compartment is the adjustable tray, stand, or holder where the solar PV module or the glass coupon rests, like the one used by Al-Hasan, who deployed a 300 × 200 mm^2 metallic stand to place glass slides on it with varying grades of tilt, all fitted inside a box for indoor dust accumulation simulation [58]. The test bench is a similar arrangement but with a more straightforward structure, in which the experiments take place without any special equipment other than a table, solar simulator, and some measurement devices, and usually dust is deposited manually [43,48,65,102,116,136]. For example, Tripathi et al. depended on a flat test bench to maintain a horizontal PV module position and a controlled indoor environment while scattering the dust with different particle sizes and fixed deposition density [18]. Fig. 26 shows a group of indoor test benches [43,48,69]. As usual, there are exceptional cases in which the researchers used different compartments rather than the test chamber or table to execute the dust accumulation simulation experiment compatible with their research needs. For example, Goossens and Van Kerschaever used a wind tunnel to examine the effect of wind speed coupled with dust soiling on the performance of PV structures [56]. A similar setup was used by Lu et al., as shown in Fig. 27 [76]. Yuan et al. were interested in investigating the effect of condensation as a replacement to water droplets on the performance of the super-hydrophobic coating, employing for that their unique test setting as demonstrated by Fig. 28 [67].

7.1.2. Solar simulator

Using an artificial light source or standard solar simulator is critical to characterize the PV modules under the effect of dust soiling, a

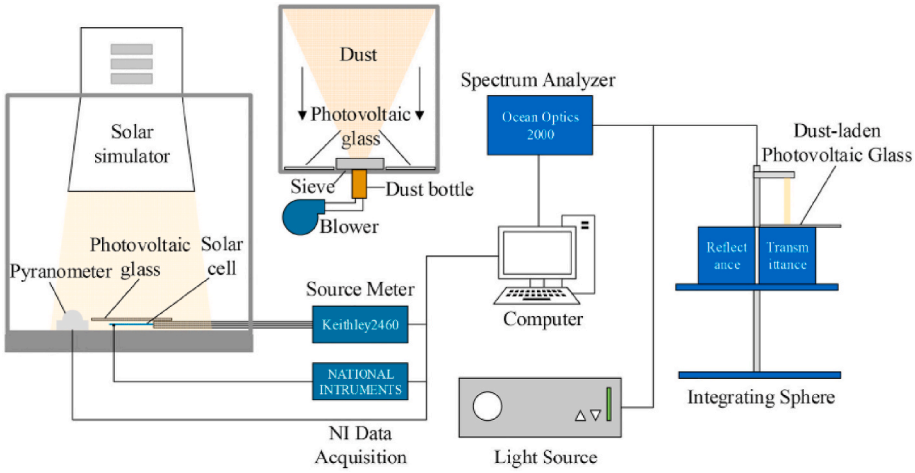

Fig. 22. Indoor experimental setup block diagram [55].

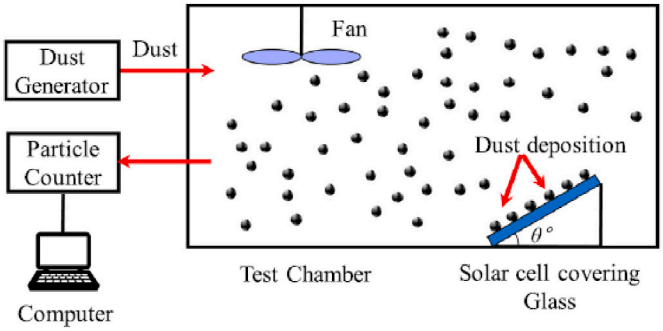

Fig. 23. Schematic design of a typical test chamber equipped with a fan for dust suspension [70,73,77].

Fig. 24. RBG 1000 dust generator manufactured by PALAS GmbH [20].

common practice that relies on an indoor experimental setup. Whether standard or not, a sun or solar simulator is a vital component of the in-house setup that secures the illumination needed for the experiment. Always Halogen, Tungsten, or Xenon lamps were deployed in the relevant studies. Fig. 29, Fig. 30, and Fig. 31 demonstrate different solar simulator types. Table 11 summarizes the different light-source solar simulators used in the relevant experimental work, while Table 12 brings the same list except for standard simulators. For light intensity measurements, pyranometers were the first choice in many studies. Table 13 lists the instruments used to measure the light intensity.

7.1.3. Sieve and particle sizer

The primary use of the sieve is to separate the dust particles according to their sizes, which is second nature among many researchers, to facilitate dispersing the targeted dust sizes on top of the PV structure or surface substrate [8,18,27,43,45,46,52,56,102]. Goossens and Van Kerschaever sieved natural aeolian dust through a 63 μm strainer [56]. Also, Yuan et al. screened artificial dust particles using a mesh with a diameter of 106 μm [67]. Fig. 32 demonstrates the sieving process dedicated to particle size analysis. Additionally, the same piece of equipment, on many occasions, was used to put down the dust layer, which dramatically helps achieve a uniform or homogenous distribution without paying much attention to the straining size or diameter [37,40,57,62,63,68,69], even though no scientific background exists to support this uniformity or homogeneity as it is randomly occurring in the natural world. An exciting presence of sieves was the vibratory type used by Sayyah et al. to obtain a smooth layer of artificial dust [50]. The particle sizer or granulometer is another standard equipment widely used in related research to help verify the different dust particle sizes [61,104,146], like the Coulter Multisizer [58] and the X-ray Malvern Mastersizer 2000 [55,67]. Fig. 33 shows a laser particle sizer manufactured by Fritsch similar to the one used by Klugmann-Radziemska in her study [61,147].

7.1.4. Glass sheet for dust collection

Several laboratory-based research depended on glass coupons seeking practicality to gather dust indoors or outdoors, determine the deposition density or concentration, or perform other relevant investigations. Menemmeche et al. used a glass piece (10 cm × 10 cm) as a simulator for the PV module to quantify dust deposition density on the PV surface after blowing the dust using compressed air from a 2-m distance [102]. The same was done by Fan et al. to find the dust concentration after depositing it on a glass sheet while having a PV module inside the same test chamber [80]. Lu et al. used tilted glass pieces within a test chamber setup displayed in Fig. 34 first to collect dust and then measure its deposition density with the assistance of weighing balance [76]. Also, the research teams compared a clear glass coupon with another coated by a super-hydrophobic coating to assess its effect on dust deposition density, which obviously decreased [70,76]. Fig. 35 pictures a clean glass plate coated by super-hydrophobic film [73], while Fig. 36 shows a couple of glass slides covered by artificial dust, part of the indoor experiment to evaluate the effect of the mentioned coating on the dust deposition density [70]. Liu et al. employed an ultra-white patterned steel glass to check the quality and examine the optical performance of this PV glass responding to the deposition density [55].

Similarly, some studies relied on the naturally gathered dust on top of PV panels or surface material slides for their indoor experimental

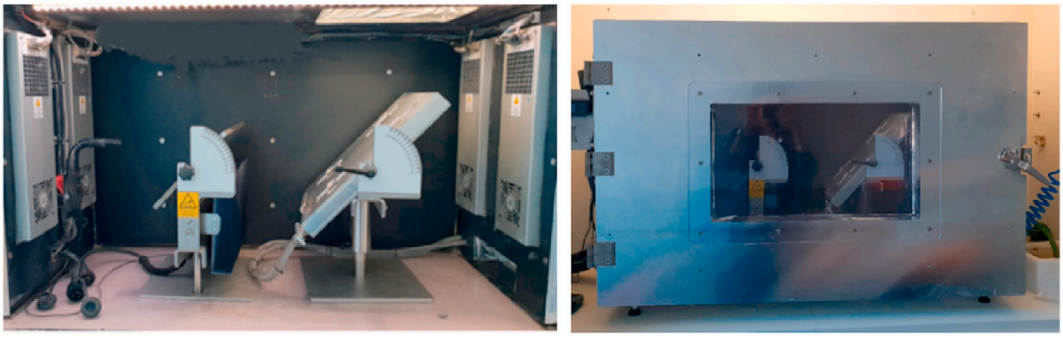

Fig. 25. CEA- INES test chamber: right) outer sight, left) inner view [78].

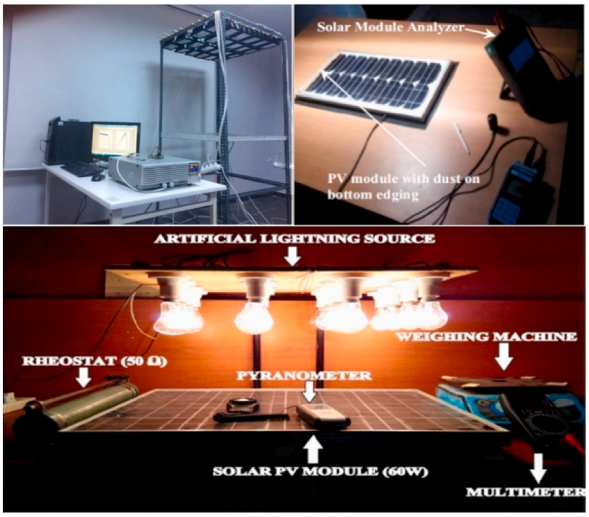

Fig. 26. Collection of Indoor test benches [43,48,69].

Fig. 27. Wind tunnel for dust removal characterization [76].

work and analysis [41]. For instance, Kazem et al. used the glass sheet to collect outdoor dust necessary for indoor experiments and, as always, to evaluate the deposition density [54]. Also, relevant researchers used a 1 m^2 glass plate to collect natural dust that will later be used in the indoor experimental work [52,115]. In contrast, Sadat et al. used a typical brush to collect their sample of natural dust that accumulated on top of panels of a small-scale PV power plant [40]. The interested scientists used heat-treated cotton to collect the dust from the PV module surface. The same cotton piece was wetted with water to collect all the dust [41,66]. An innovative method was followed by Qasem et al., in which they

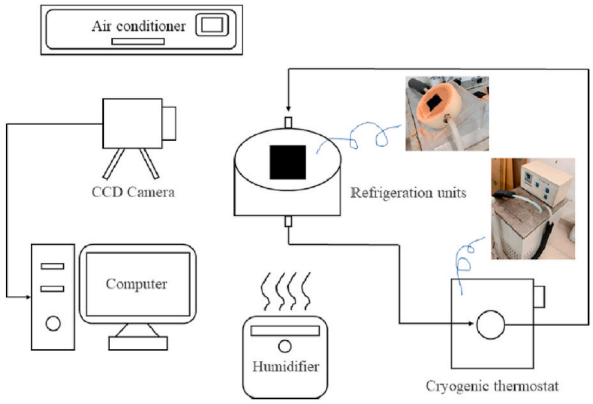

Fig. 28. Condensation visualization platform to test the dust removal characteristics of the super-hydrophobic coating [67].

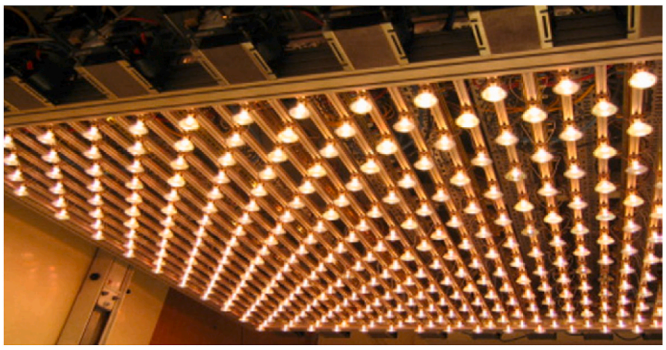

Fig. 29. Solar simulator [16].

used a collecting vessel to gather dust after being left outdoors for several days. Then, a glass plate was present for picking dust particles [92].

7.1.5. *Weighing balance*

The weighing balance is always related to quantifying the collected dust amounts, leading to calculating the dust deposition density [41,43,66]. The researchers used various models, including precision, electronic, and digital weighing scales [57,69,74,75]. While Fig. 37 provides a photograph of an electronic balance, Table 14 lists the balance technologies and their relevant models used again within the studies covered by this article. Of course, there were cases in which the scientists depended on unconventional techniques to evaluate the deposition density, like the work of Al-Maghalseh, who used a dust sensor to obtain the relevant density [81].

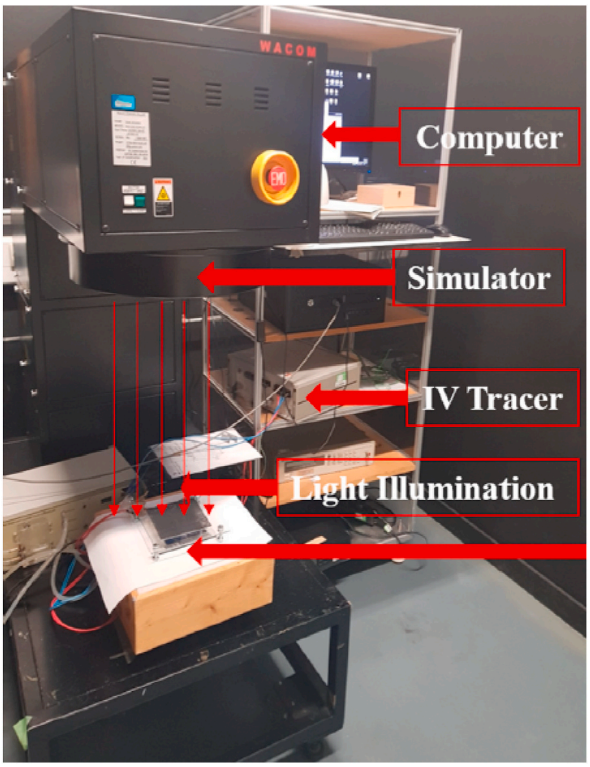

Fig. 30. Wacom solar simulator [27].

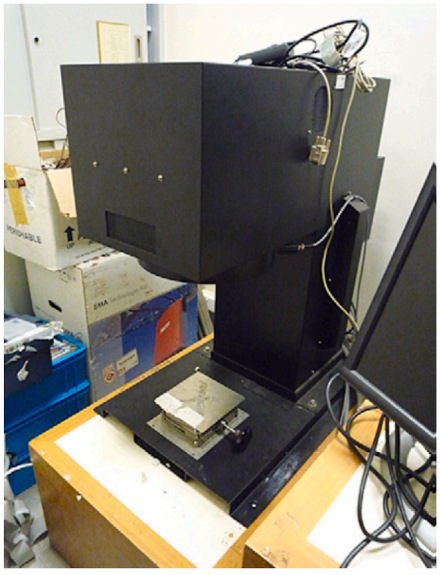

Fig. 31. Xenon lamp solar simulator [16].

7.1.6. Particle counter

Usually attached to the test chamber, the particle counter identifies a specific dust particle size's concentration, distribution, and deposition density [152]. Of course, dust concentration is vital because it affects the transmittance of the PV glazing [153] and helps assess the quality of the self-cleaning coating, but few studies used it [16,64,70,73,76,77]. Fig. 38 shows the OLS4031 optical particle counter manufactured by PAMAS [154], while Fig. 39 illustrates some results obtained by another particle counter, as provided by Zhang et al. [73].

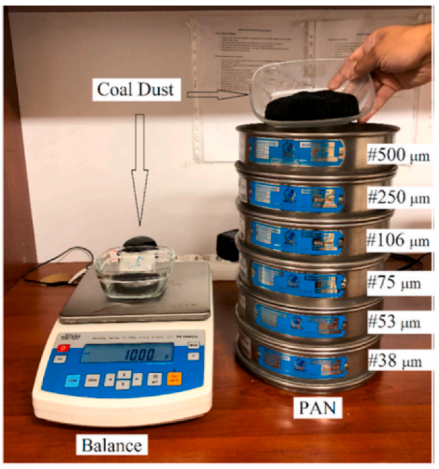

Fig. 32. Coal dust samples preparation [43].

7.2. Dust deposition techniques

Researchers used different approaches to dispense dust particles and manage a uniform distribution on top of the designated surfaces [48,68]. In contrast, others did not pay attention to the uniformity of dust dispersal, either by not practically laying a uniform film of dust or simply not discussing uniformity in their work [18,59]. In principle, two dust deposition mechanisms are there: dry and wet deposition. Piedra et al. used a deposition chamber, where pressurized air injected dust from a flask. Fig. 40 displays a schematic of that test chamber [84], while Fig. 41 shows a realistic photograph of a similar dust deposition chamber [72]. Also, many researchers used blowers integrated with dust vessels to fill the test chamber with dust particles. For instance, Al-Hasan used a blower fixed on the front side of a box to scatter dust particles on an inclined glass coupon [58]. The research conducted by Abderrezek and Fathi used an air compressor to disperse soil particles on top of a glass coupon with a particle size of 100–300 μm [51]. Menemmeche et al. made a 2-m distance between the air compressor and the PV module, guaranteeing a uniform settlement of dust on top of the module [102]. Guo et al. called the dust scattering mechanism followed by their illustrated system in Fig. 42 "aerosol deposition," which employed an aerosol generator and air compressor to inject the test chamber with the flying dust. The team of Sisodia and Mathur applied uniform layers of dust samples on top of the PV module inside the test chamber using a strainer with a sieve identical to the particle size [63]. Again, Sadat et al. relied on the manual sieving process to homogeneously scatter the dust particles on top of the test PV panel, this time with a strainer having a bigger diameter (i.e., 10 cm) [40]. Fig. 43 shows a PV module covered by a homogenous layer of carbon dust applied using the manual sieving technique as part of the indoor testing-based study done by Darwish et al. [68]. Garcia et al. used an innovative test chamber in which pre-mixed dust with pressurized air enters the space from a diffuser with a built-in deflector in the form of a homogenous cloud [78]. Also, Goossens and Van Kerschaever used a dust-cloud producer developed by the Engelhardt laboratory to inject dust inside a wind tunnel as part of their experimentation [56]. Adversely, Sayyah et al. used a vibratory sieve to deposit their artificial dust on the surface substrate prototype [50].

Another approach followed by many researchers is that they depend on outdoor exposure of PV modules or glass substrates for natural dust deposition. Afterward, a group of tests would be applied over the surface after moving it indoors without further dust agglomeration [108,115]. In confirmation of this, Klugmann-Radziemska and Rudnicka put four PV panels outdoors to collect dust and evaluated their monthly performance by moving them inside a test chamber [62]. Considering the wettability of the deposition process, some researchers sprayed dust and water mixture on their PV module before placing the panel inside the

Table 11
A summary of artificial light sources used in the reviewed literature.

Reference	Artificial light source	Experimental light intensity (W/m^2)	Power (W per lamp)
[117]	halogen lamp	200–800	–
[114]		987	–
[62]		1000	1000
[56]		1000	• 1000 • 500
[63]		–	650
[43]		1000	500
[103]	high-power halogen lamp	–	–
[85]	Tungsten lamp	–	100
[49]		• 276.6 • 553.3 • 830 • 1106	0–500
[116]		• 211 • 384 • 576 • 893	1000
[17]	Tungsten–halogen	• 400 • 195	1000
[52]		850	1600
[58]		–	1200
[68]		600	500
[16]	Xenon lamp	–	–
[61]		–	–
[72]	high-voltage xenon lamp	500 per lamp	–
[18]	incandescent bulb	449–920	• 100 • 200
[86]		• 567 • 1024	
[137]		• –	–
[71]	Spotlight	• 340 • 301 • 255	• 500
[88]		340	100
[48]	• LED • Halogen lamps		• 15 • 500
[57]	Heliocentris solar lamp	1000	–
[80]	adjustable light source	0–350	1000
[47]	Constant light source	–	–
[65]	White flood light	• –	• –
[102]	Light bulb	• –	500
[59]		• 500	• –
[74,75]	Solar lamp	• –	• –
[57]		1000	–
[69]	lightning setup	• 650 • 750 • 850	100
[45]	MINI-EESTC thermal solar energy basic unit	• 200 • 400 • 600 • 800 • 1000	50

Table 12
A list of standard solar simulators used in the reviewed literature.

Reference	Solar simulator	Manufacturer	Class	Experimental light intensity (W/m^2)
[41,66]	SPI-SUN 5600SLP BLUE	Eternalsunspire	A + [127]	
[37]	SEC 1100	Atlas	–	1000
[55]	LASI-1	Sciencetech	C [138]	300–1300
[27]	Wacom Continuous	Wacom Electric	–	–
[40]	SolSim 2	Luzchem	–	–
[78]	Pasan	–	A	–
[16]	Solar simulator	–	–	0–1000
[54]		–	–	600
[81]		–	–	1000
[64]		–	–	950
[115]		–	–	0–800
[44]		–	–	

Table 13
List of instruments for light-intensity measurements used in the reviewed studies.

Reference	equipment	model	Manufacturer	Uncertainty
[68]	Pyranometer	–	–	–
[49]		–	–	–
[116]		–	–	–
[55]		CMP 10	Kipp & Zonen	2 % [139]
[60]		CMP 6		6 % [140]
[8]		Li-Cor		–
[61]		SP Lite2		–
[37]		CMP 6		6 % [140]
[17]		SPP	Eppley	1–2 % [141]
[45]		WE300	YSI	1 % [142]
[63]	Solar power meter	–	–	–
[18]		–	–	–
[115]		TM-206	TENMARS	> ±5 % [143]
[117]				3–5 % [143]
[58]		HAENNI Solar 118	–	–
[54]		MT-4617	Pro'sKit	±0.3 %
[69]		DT-1307	CEM	±5 % [144]
[72]		–	–	–
[62]		METEON	Kipp & Zonen	0.1 %
[56]	Laser Power-Energy Monitor	Ophir Nova	Ophir Nova	±3 % [145]
[57]	Solar irradiance	–	–	–
[114]	sensor	–	–	–
[71]	Photo-radiometer	HD2302	Delta OHM	–
[88]		dHD 9221	Delta OHM	–

indoor setup [41,66]. Liu et al. prepared an anhydrous ethanol and dust mixture, which was later sprayed on the PV surface because of ethanol's volatility to ensure no humidity left [55]. Table 15 lists the primary dust deposition techniques followed by the scientists in the reviewed literature. Subsequently, the mentioned dust deposition techniques can be categorized into automatic, manual, and outdoor exposure categories according to the particle launching mechanisms. The flowchart delivered in Fig. 44 lists the different machinery in each category.

8. Systematic method

In this section, we analyze and interpret the comprehensive categorized information provided in the previous sections to develop or extract a generic workflow that guides all future work interested in studying dust's effect on PV performance based on laboratory experiments.

Fig. 33. Next Nano ANALYSETTE 22 laser particle sizer by Fritsch [147].

Therefore, Fig. 45 shows a flowchart of the systematic technique or pattern we devised for indoor dust deposition experiments based on our observations while writing this review paper. The flowchart starts with identifying and gathering the dust samples. These samples' physical and chemical properties are then ascertained using the proper tools (e.g.,

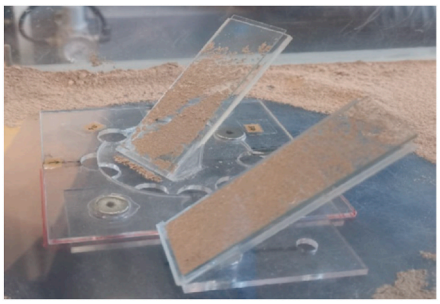

Fig. 34. Tilted dusty glass coupon inside a test chamber [76].

Fig. 35. Super-hydrophobic coated glass sheet [73].

Fig. 36. Coated (right) and Uncoated (left) glass slides covered by A2 Test dust (ISO 12103-1) [70].

SEM, EDX). The PV module's dust removal, optical, electrical, and thermal properties are then determined through laboratory tests, mainly using solar simulators and test chambers to imitate the natural dust formation mechanism. It is worth noting that this deduced framework matches a tangible model or pattern detected in every laboratory-based work reviewed in the current effort. It is also essential that we list the necessary tools and apparatus that were used to perform all the different types of experimental activities mentioned throughout the article. Hence, Table 16 brings this list, which represents part of the practical added value of the article, as specialized researchers can directly resort to it while searching for a specific testing process and its corresponding piece of equipment.

Fig. 37. Electronic balance [8].

Table 14
List of balances used in the reviewed literature.

Reference	Balance type	Balance model	Readability	Uncertainty
[50]	Analytical Balance	Cole-Parmer Symmetry	–	–
[27]		Mettler Toledo ME204	0.1 mg [148]	–
[69]	Balance	–	–	–
[37]		–	1 g	–
[43]		–	–	–
[56]		Mettler Toledo PJ3000	0.01 [149]	0.001 g
[92]		–	–	0.1 mg
[104]		Sartorius BSA2245-CW	–	0.0001 g
[41,66]	Digital analytical balance	–	–	–
[102]	Digital balance	–	–	–
[115]	Digital balance	AGROMER	–	0.01 %
[55]	Electronic balance	–	–	–
[57]		Scientech	–	±0.0001 g
[80]		Sartorius BT 125D	–	±0.00001g [150]
[40]		Sartorius Entris	0.1 mg	–
[54]	Sensitive weight type Delicate balance	EJ6I0-E	–	0.36 %
[48]	Precision electronic balance	Ohaus Scout Pro SPU602	0.01 g	–
[63]	High-precision digital balance	Amici tools, 8068 series	0.001 mg	–
[46]	Precision balance	Sartorius MC-210S	0.01 mg	–
[8]		–	–	0.1 mg
[72]		–	–	0.0001 mg
[77]		FX-2001IWP		–
[76]				
[73]				
[70]		–	–	–
[78]		–	–	–
[75]	Precision microbalance	Precisa 4SM-200A	0.01 mg [151]	±0.1 mg [151]
[74]				
[17]		–	1 μg	–

9. Conclusion

Many recent studies tackled and quantified the impact of dust soiling based on outdoor exposure on PV panels [156–158]. Accordingly, different results were produced depending on the location, the tilt angle, and the PV technology used. Still, all agreed upon the deteriorating

Fig. 38. PAMAS OLS4031 optical particle counter [154].

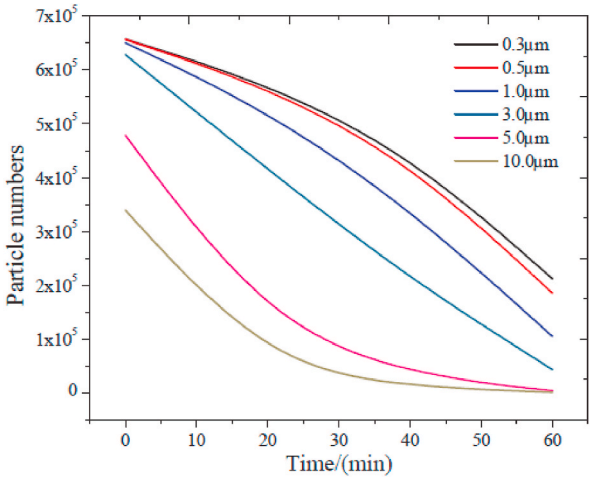

Fig. 39. Dust concentration per particle size during the deposition process [73].

effect of dust buildup on the PV performance. From an opposite angle, the present study thoroughly categorized, reported, and explained the different laboratory-based experimental practices that the investigators relied on to examine the effects of dust deposition on PV electrical, optical, thermal, and surface-adhesion characteristics. A flowchart of a

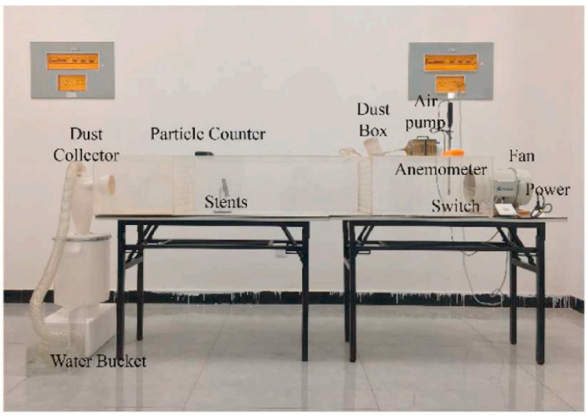

Fig. 41. Photographic view of a dust deposition chamber [72].

systematic technique, or pattern, for dust deposition indoor experiments was developed. Also, a list of the most typically used equipment was provided. The importance of this effort lies in the fact that it collected all possible indoor methods in one place, thus enabling future researchers to have a holistic view of how to conduct this type of experiment inside the laboratory. Of course, the literature is rich in relevant content, but it is scattered and has not yet been composed in this manner as far as it comes to our knowledge. The main challenge facing the PV dust deposition research based on indoor practices, which was observed during the construction of this work, is that many laboratories have limited access to high-precision equipment intended for scientific experimentation, resulting in subsequent detectable differences in the obtained results. Finally, the following concluding remarks exhibit the milestones of this study:

1. It has been noticed that researchers tend to use artificial dust more in indoor experiments than naturally sourced, which was mainly collected from the local environment. The most commonly used synthetic dust was ISO 12103-1 A2 Test dust, manufactured by Powder Technology Inc, USA, with a 1–125 μm particle size.
2. SEM imaging technique was widely used in systematic indoor experimental work to examine the topography of dust particles.
3. The indoor testing setups, like the test chamber and test bench, were used to help investigate the effect of dust deposition on the designated characteristics of the PV devices and deposition surfaces. The earlier setup is usually equipped with a dust generator, while the latter, a primitive version of the same arrangement, depends on manual methods for dust deposition.
4. A glass slide was usually placed inside a test chamber with different inclinations or horizontally on a test bench to identify its

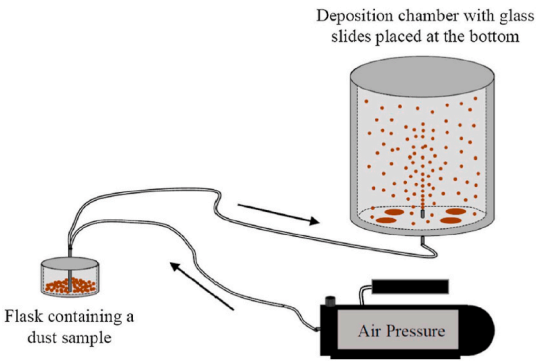

Fig. 40. A schematic of a dust generator and test chamber [84].

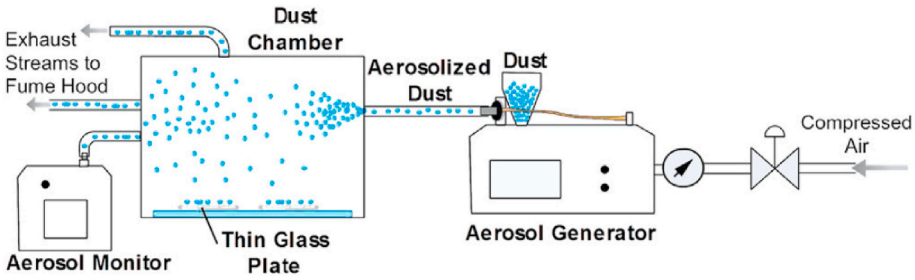

Fig. 42. Aerosol deposition system [107].

Fig. 43. Uniformly distributed carbon dust on a PV module [68].

Table 15
Summary of the leading dust deposition techniques used in the reviewed literature.

Reference	Dust deposition mechanism
[17,44,54,55,80]	Blower
[92]	Collecting vessel
[84,102]	Compressed air
[56]	Dust cloud producer
[16,64,70,72,73,77]	Dust generator and fan
[58,67,74–76,78,84,85]	Dust Generator
[81–83,155]	Fan
[27,46,92]	Manual free fall through a dispenser
[18,43,45,47,48,53,59,65,71,88,114]	Manual scattering
[52,115]	Manual scattering and vibration
[61,62,117]	Outdoor deposition
[79]	Powder gun
[37,40,57,63,68,69,86]	Sieve or Strainer
[8,41,60,66]	Spraying procedure
[50,105]	Vibratory sieve

optical and dust removal characteristics and quantify the dust deposition density.

5. For the electrical description of PV modules under the known indoor testing conditions here, the researchers usually sought to measure either the current and voltage or the I–V curve characteristics. It is critical in many cases to use external resistance (variable or fixed) in the measuring system. The rule of thumb is that variable loads accompany the I–V characteristics measurements, while the fixed loads are assigned to voltage and current readings.
6. The thermal characterization of PV modules was also considered in many studies depending on temperature sensors (e.g., thermocouples and RTD) to measure surface, backside, and ambient temperatures.
7. In many studies, the indoor conditions were controlled through an air conditioning system to ensure no undesirable influence of temperature and humidity was present.
8. Different solar simulator types were used to stand for the light source needed for the indoor experiments. The Halogen and Xenon lamps solar simulators were the most commonly used, along with the standard types produced by manufacturers. Pyranometers and solar power meters were used the most for light intensity measurements.
9. The sieve was commonly used to separate the different dust particle sizes. The same equipment was often used to help uniformly disperse dust on top of a particular surface. In a more advanced fashion, a particle sizer was used to accomplish the same function of size analysis.
10. On some occasions, the researchers resorted to the particle counter to specify the concentration, distribution, and deposition density of specific particle sizes.

10. Recommendations for future work

1. It is recommended that the investigators use different PV technologies from the silicon-based ones in laboratory-based experiments to study their reaction to the presence of dust.
2. It is recommended that the research teams use more sophisticated and high-precision equipment to reinforce the reliability of their research outcomes.
3. It is recommended that the researchers follow the suggested systematic framework here as a guideline to sequentially employ the needed characterizations for their future work regardless of the available equipment or measuring devices because this necessarily varies from one laboratory to another.
4. It is recommended to conduct research combining indoor and outdoor experiments to facilitate more comparison between relevant

Table 16
List of the leading experimental activities and their corresponding equipment.

Experimental Activity	Equipment	Description	Function
All indoor dust investigation activities	PV module	Crystalline silicon technology	Study material
	Deposition surface	Low-iron glass or acrylic plastic sheet	
	Dust material	Artificial or Natural	
Morphological characterization	SEM		Identify the shape of dust particles and their sizes.
	Microscope	Digital, electron, optical, regular	
	CCD camera	–	
	Particle sizer	Laser	Identify dust particle size
Mineralogical characterization	XRF	Natural dust	Identify the chemical composition of dust
	XRD		
Elemental characterization	EDS or EDX	Natural or artificial dust	Identify dust chemical composition elementwise
Dust deposition	Test chamber	Standard or custom-made	Artificially deposit dust on the PV module or the deposition surface
	Dust generator		
	Test bench	–	
Artificial illumination	Solar simulator	Standard or custom-made (Halogen, Tungsten, Xenon, LED, Spotlight, Tungsten-Halogen, etc.)	Light source
Dust removal	Adjustable tray	Generally placed inside the test chamber	Controls the tilt angle to remove the dust
	Self-cleaning coating	Hydrophobic and super hydrophobic	Passive dust removal
	EDS coating	Under test	Active dust removal
	Wind tunnel chamber	–	Blowing away dust using airstreams
Optical characterization	Spectrophotometer	UV, UV-VIS, UV/VIS/NIR	Identify the transmittance of the PV or deposition surface
Electrical characterization	Multimeter	Analog, digital, universal digital	Current and voltage
	Voltmeter	Digital	
	External resistance (load)	Fixed load	
	Current and voltage sensors	–	
	Ammeter	Digital	
	Multivoltmeter	–	
	I–V tracer	–	I–V and P–V curves
	External resistance (load)	Variable load	.
	Current and voltage sensors	–	
	Source measure unit	–	
	Oscilloscope	–	
Thermal characterization	Temperature sensor	- Thermocouple (K-type, T-type) - RTD (PT100)	Surface, backside, and ambient temperatures
	Thermometer	Digital, infrared	
Light intensity	Pyranometer	–	Solar irradiance
	Solar power meter	–	
	Solar irradiance sensor	–	
	Photo-radiometer	–	
	Laser power-energy monitor	–	
Dust accumulation	Sieve	Manual, vibratory	Dust scattering
Dust deposition density	Weighing balance	Analytical, digital, precision	Weighing of dust and collection surface pre and post-deposition
	Particle counter	Optical	Deposition density and dust particle size concentration

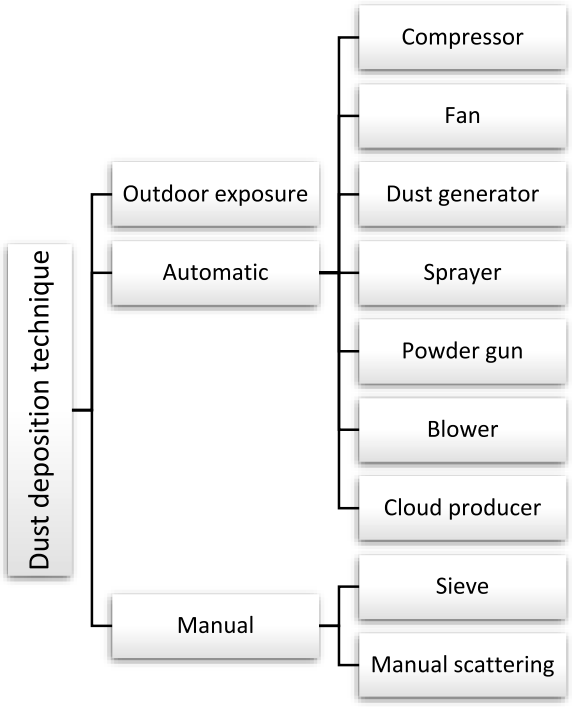

Fig. 44. Classification of dust deposition techniques and equipment.

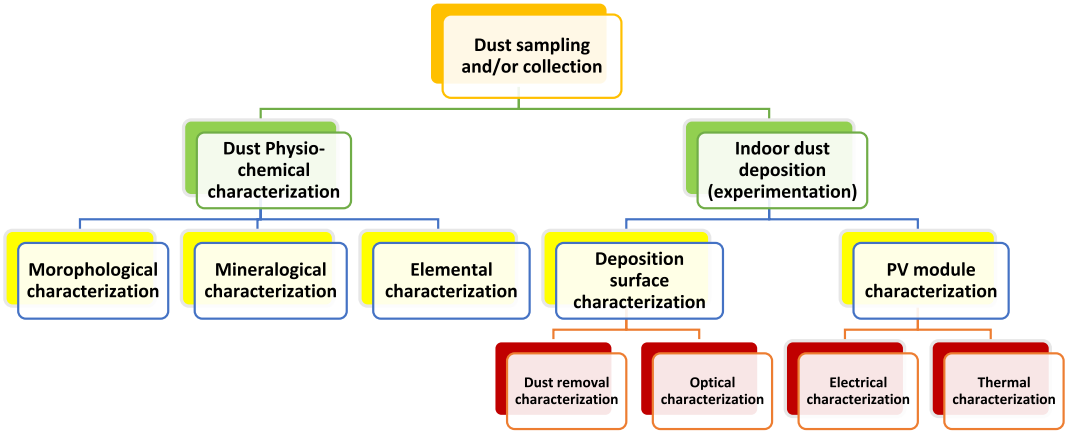

Fig. 45. Flowchart of systematic indoor experimental research for testing dust deposition effect.

results to strengthen the laboratory experimental practices based on the real-world scenario.

5. It is recommended that the researchers work on deriving an empirical mathematical term to be added to the solar cell equivalent circuit models to represent the dust accumulation effect, which, from an initial perspective, can be done given that the layer of dust directly affects the cell's electrical current, which is always the dependent variable in the mentioned equations.

Declaration of competing interest

The authors declare the following financial interests/personal relationships which may be considered as potential competing interests: Abubaker Younis reports a relationship with Transilvania University of Brasov that includes: employment.

Data availability

No data was used for the research described in the article.

References

[1] IRENA, Country Rankings. https://www.irena.org/Data/View-data-by-topic/Capacity-and-Generation/Country-Rankings, 2023. (Accessed 16 April 2023).
[2] IRENA, Energy Profile-China, 2022.
[3] IRENA, Energy Profile-Germany, 2022, https://doi.org/10.1351/goldbook.e02112.
[4] K. Ilse, M.Z. Khan, N. Voicu, V. Naumann, C. Hagendorf, J. Bagdahn, Advanced performance testing of anti-soiling coatings – Part I: Sequential laboratory test methodology covering the physics of natural soiling processes, Sol. Energy Mater. Sol. Cells 202 (2019) 110048, https://doi.org/10.1016/j.solmat.2019.110048.
[5] K. Menoufi, Dust accumulation on the surface of photovoltaic panels: introducing the photovoltaic soiling index (PVSI), Sustainability 9 (2017), https://doi.org/10.3390/su9060963.
[6] T. Sarver, A. Al-Qaraghuli, L.L. Kazmerski, A comprehensive review of the impact of dust on the use of solar energy: history, investigations, results, literature, and mitigation approaches, Renew. Sustain. Energy Rev. 22 (2013) 698–733, https://doi.org/10.1016/j.rser.2012.12.065.

[7] P.K. Enaganti, A. Bhattacharjee, A. Ghosh, Y.N. Chanchangi, C. Chakraborty, T. K. Mallick, S. Goel, Experimental investigations for dust build-up on low-iron glass exterior and its effects on the performance of solar PV systems, Energy 239 (2022) 122213, https://doi.org/10.1016/j.energy.2021.122213.

[8] J.K. Kaldellis, P. Fragos, M. Kapsali, Systematic experimental study of the pollution deposition impact on the energy yield of photovoltaic installations, Renew. Energy 36 (2011) 2717–2724, https://doi.org/10.1016/j.renene.2011.03.004.

[9] A. Juaidi, H.H. Muhammad, R. Abdallah, R. Abdalhaq, A. Albatayneh, F. Kawa, Experimental validation of dust impact on-grid connected PV system performance in Palestine: an energy nexus perspective, Energy Nexus 6 (2022) 100082, https://doi.org/10.1016/j.nexus.2022.100082.

[10] A. Hosseini, M. Mirhosseini, R. Dashti, Analytical study of the effects of dust on photovoltaic module performance in Tehran, capital of Iran, J. Taiwan Inst. Chem. Eng. (2023) 104752, https://doi.org/10.1016/j.jtice.2023.104752.

[11] G.A. Mastekbayeva, S. Kumar, Effect of dust on the transmittance of low density polyethylene glazing in a tropical climate, Sol. Energy 68 (2000) 135–141.

[12] W.J. Jamil, H. Abdul Rahman, S. Shaari, Z. Salam, Performance degradation of photovoltaic power system: review on mitigation methods, Renew. Sustain. Energy Rev. 67 (2017) 876–891, https://doi.org/10.1016/j.rser.2016.09.072.

[13] H.Z. Al Garni, The impact of soiling on PV module performance in Saudi arabia, Energies 15 (2022) 1–25.

[14] Z. Song, J. Liu, H. Yang, Air pollution and soiling implications for solar photovoltaic power generation: a comprehensive review, Appl. Energy 298 (2021) 117247, https://doi.org/10.1016/j.apenergy.2021.117247.

[15] K.K. Ilse, B.W. Figgis, V. Naumann, C. Hagendorf, J. Bagdahn, Fundamentals of soiling processes on photovoltaic modules, Renew. Sustain. Energy Rev. 98 (2018) 239–254, https://doi.org/10.1016/j.rser.2018.09.015.

[16] H. Jiang, L. Lu, K. Sun, Experimental investigation of the impact of airborne dust deposition on the performance of solar photovoltaic (PV) modules, Atmos. Environ. 45 (2011) 4299–4304, https://doi.org/10.1016/j.atmosenv.2011.04.084.

[17] M.S. El-Shobokshy, F.M. Hussein, Degradation of photovoltaic cell performance due to dust deposition on to its surface, Renew. Energy 3 (1993) 585–590, https://doi.org/10.1016/0960-1481(93)90064-N.

[18] A.K. Tripathi, M. Aruna, E.P. Venkatesan, M. Abbas, A. Afzal, S. Shaik, E. Linul, Quantitative analysis of solar photovoltaic panel performance with size-varied dust pollutants deposition using different machine learning approaches, Molecules 27 (2022), https://doi.org/10.3390/molecules27227853.

[19] S. Fan, X. Wang, S. Cao, Y. Wang, Y. Zhang, B. Liu, A novel model to determine the relationship between dust concentration and energy conversion efficiency of photovoltaic (PV) panels, Energy 252 (2022) 123927, https://doi.org/10.1016/j.energy.2022.123927.

[20] F.M. Zaihidee, S. Mekhilef, M. Seyedmahmoudian, B. Horan, Dust as an unalterable deteriorative factor affecting PV panel's efficiency: why and how, Renew. Sustain. Energy Rev. 65 (2016) 1267–1278, https://doi.org/10.1016/j.rser.2016.06.068.

[21] H.A. Kazem, M.T. Chaichan, A.H.A. Al-Waeli, K. Sopian, A review of dust accumulation and cleaning methods for solar photovoltaic systems, J. Clean. Prod. 276 (2020) 123187, https://doi.org/10.1016/j.jclepro.2020.123187.

[22] I. Al Siyabi, A. Al Mayasi, A. Al Shukaili, S. Khanna, Effect of soiling on solar photovoltaic performance under desert climatic conditions, Energies 14 (2021).

[23] N. Ammari, M. Mehdi, A. Alami Merrouni, H. El Gallassi, E. Chaabelasri, A. Ghennioui, Experimental study on the impact of soiling on the modules temperature and performance of two different PV technologies under hot arid climate, Heliyon 8 (2022) e11395, https://doi.org/10.1016/j.heliyon.2022.e11395.

[24] Asad Ullah, A. Amin, T. Haider, M. Saleem, N. Zafar, Investigation of soiling effects , dust chemistry and optimum cleaning schedule for PV modules in Lahore , Pakistan, Renew. Energy 150 (2020) 456–468, https://doi.org/10.1016/j.renene.2019.12.090.

[25] M. Memiche, C. Bouzian, A. Benzahia, A. Moussi, Effects of dust, soiling, aging, and weather conditions on photovoltaic system performances in a Saharan environment—case study in Algeria, Glob. Energy Interconnect. 3 (2020) 60–67, https://doi.org/10.1016/j.gloei.2020.03.004.

[26] A. Younis, Y. Alhorr, Modeling of dust soiling effects on solar photovoltaic performance: a review, Sol. Energy 220 (2021) 1074–1088, https://doi.org/10.1016/j.solener.2021.04.011.

[27] Y.N. Chanchangi, A. Ghosh, S. Sundaram, T.K. Mallick, An analytical indoor experimental study on the effect of soiling on PV, focusing on dust properties and PV surface material, Sol. Energy 203 (2020) 46–68, https://doi.org/10.1016/j.solener.2020.03.089.

[28] Y.N. Chanchangi, A. Ghosh, H. Baig, S. Sundaram, T.K. Mallick, Soiling on PV performance influenced by weather parameters in Northern Nigeria, Renew. Energy 180 (2021) 874–892, https://doi.org/10.1016/j.renene.2021.08.090.

[29] S. Ghazi, A. Sayigh, K. Ip, Dust effect on flat surfaces - a review paper, Renew. Sustain. Energy Rev. 33 (2014) 742–751, https://doi.org/10.1016/j.rser.2014.02.016.

[30] T. Zarei, M. Abdolzadeh, M. Yaghoubi, Comparing the impact of climate on dust accumulation and power generation of PV modules: a comprehensive review, Energy Sustain. Dev. 66 (2022) 238–270, https://doi.org/10.1016/j.esd.2021.12.005.

[31] M. Jaszczur, Q. Hassan, K. Styszko, J. Teneta, Impact of dust and temperature on energy conversion process in photovoltaic module, Therm. Sci. 23 (2019) 1190–1210, https://doi.org/10.2298/TSCI19S4199J.

[32] A. Gholami, M. Ameri, M. Zandi, R.G. Ghoachani, S. Eslami, S. Pierfederici, Photovoltaic potential assessment and dust impacts on photovoltaic systems in Iran: review paper, IEEE J. Photovoltaics 10 (2020) 824–837, https://doi.org/10.1109/JPHOTOV.2020.2978851.

[33] K.R.C. Lakshmi, G. Ramadas, Dust deposition's effect on solar photovoltaic module performance: an experimental study in India's tropical region, J. Renew. Mater. 10 (2022) 2133–2153, https://doi.org/10.32604/jrm.2022.019649.

[34] M.M. Fraga, B.L. de O. Campos, T.B. de Almeida, J.M.F. da Fonseca, V. de F. C. Lins, Analysis of the soiling effect on the performance of photovoltaic modules on a soccer stadium in Minas Gerais, Brazil, Sol. Energy 163 (2018) 387–397, https://doi.org/10.1016/j.solener.2018.02.025.

[35] F.A. Mejia, J. Kleissl, Soiling losses for solar photovoltaic systems in California, Sol. Energy 95 (2013) 357–363, https://doi.org/10.1016/j.solener.2013.06.028.

[36] A. Khodakaram-Tafti, M. Yaghoubi, Experimental study on the effect of dust deposition on photovoltaic performance at various tilts in semi-arid environment, Sustain. Energy Technol. Assessments 42 (2020) 100822, https://doi.org/10.1016/j.seta.2020.100822.

[37] A. Younis, M. Onsa, Y. Alhorr, E. Elsarrag, Development of an empirical coefficient for the short circuit current to determine soiling effect on PV performance, Univ. KHARTOUM Eng. J. 7 (2017) 34–40. http://ejournals.uofk.edu/index.php/kuej/article/view/1581.

[38] O. Güngör, H. Kahveci, H.S. Gökçe, The effect of various industrial dust particles on the performance of photovoltaic panels in Turkey, Environ. Sci. Pollut. Res. 30 (2023) 15128–15144, https://doi.org/10.1007/s11356-022-23216-0.

[39] S. Boppana, V. Rajasekar, G. Tamizhmani, Working towards the development of a standardized artificial soiling method, in: IEEE 42nd Photovolt. Spec. Conf. PVSC 2015, IEEE, 2015, https://doi.org/10.1109/PVSC.2015.7355987.

[40] S.A. Sadat, J. Faraji, M. Nazififard, A. Ketabi, The experimental analysis of dust deposition effect on solar photovoltaic panels in Iran's desert environment, Sustain. Energy Technol. Assessments 47 (2021) 101542, https://doi.org/10.1016/j.seta.2021.101542.

[41] J. Tanesab, D. Parlevliet, J. Whale, T. Urmee, The effect of dust with different morphologies on the performance degradation of photovoltaic modules, Sustain. Energy Technol. Assessments 31 (2019) 347–354, https://doi.org/10.1016/j.seta.2018.12.024.

[42] Z.A. Darwish, H.A. Kazem, K. Sopian, M.A. Al-Goul, H. Alawadhi, Effect of dust pollutant type on photovoltaic performance, Renew. Sustain. Energy Rev. 41 (2015) 735–744, https://doi.org/10.1016/j.rser.2014.08.068.

[43] E. Adıgüzel, E. Özer, A. Akgündoğdu, A. Ersoy Yılmaz, Prediction of dust particle size effect on efficiency of photovoltaic modules with ANFIS: an experimental study in Aegean region, Turkey, Sol. Energy. 177 (2019) 690–702, https://doi.org/10.1016/j.solener.2018.12.012.

[44] M.T. Chaichan, H.A. Kazem, Effect of sand , ash and soil on photovoltaic performance : an experimental study, Int. J. Sci. Eng. Sci. 1 (2017) 22–32.

[45] M.T. Chaichan, H.A. Kazem, Experimental evaluation of dust composition impact on photovoltaic performance in Iraq, Energy Sources, Part A Recover, Util. Environ. Eff. (2020) 1–22, https://doi.org/10.1080/15567036.2020.1746444.

[46] N.S. Beattie, R.S. Moir, C. Chacko, G. Buffoni, S.H. Roberts, N.M. Pearsall, Understanding the effects of sand and dust accumulation on photovoltaic modules, Renew. Energy 48 (2012) 448–452, https://doi.org/10.1016/j.renene.2012.06.007.

[47] K.I. Abass, D.S. M Al-Zubaidi, A.A.K. Al-Waeli, Effect of pollution and dust on PV performance, Int. J. Civil, Mech. Energy Sci. 3 (2017) 181–185, https://doi.org/10.24001/ijcmes.3.4.1.

[48] M. Abderrezek, M. Fathi, Experimental study of the dust effect on photovoltaic panels' energy yield, Sol. Energy 142 (2017) 308–320, https://doi.org/10.1016/j.solener.2016.12.040.

[49] Z.A. Darwish, K. Sopian, H. Alawadhi, H.A. Kazem, M.A. Alghoul, The impact of calcium carbonate on the photovoltaic performance: an indoor experimental study, Int. J. Appl. Eng. Res. 11 (2016) 2091–2097.

[50] A. Sayyah, D.R. Crowell, A. Raychowdhury, M.N. Horenstein, M.K. Mazumder, An experimental study on the characterization of electric charge in electrostatic dust removal, J. Electrostat. 87 (2017) 173–179, https://doi.org/10.1016/j.elstat.2017.04.001.

[51] M. Abderrezek, M. Fathi, Effect of dust deposition on the performance of thin film solar cell, Elektron. IR ELEKTROTECHNIKA. 24 (2018) 41–45.

[52] H.A. Kazem, M.T. Chaichan, Experimental analysis of the effect of dust's physical properties on photovoltaic modules in Northern Oman, Sol. Energy 139 (2016) 68–80, https://doi.org/10.1016/j.solener.2016.09.019.

[53] H. Kawamoto, B. Guo, Improvement of an electrostatic cleaning system for removal of dust from solar panels, J. Electrostat. 91 (2018) 28–33, https://doi.org/10.1016/j.elstat.2017.12.002.

[54] H.A. Kazem, M.T. Chaichan, A.H.A. Al-Waeli, K. Sopian, Effect of dust and cleaning methods on mono and polycrystalline solar photovoltaic performance: an indoor experimental study, Sol. Energy 236 (2022) 626–643, https://doi.org/10.1016/j.solener.2022.03.009.

[55] L. Liu, H. Qian, E. Sun, B. Li, Z. Zhang, B. Miao, Z. Li, Power reduction mechanism of dust-deposited photovoltaic modules: an experimental study, J. Clean. Prod. 378 (2022) 134518, https://doi.org/10.1016/j.jclepro.2022.134518.

[56] D. Goossens, E. Van Kerschaever, Aeolian dust deposition on photovoltaic solar cells: the effects of wind velocity and airborne dust concentration on cell performance, Sol. Energy 66 (1999) 277–289, https://doi.org/10.1016/S0038-092X(99)00028-6.

[57] A.A. Hachicha, I. Al-sawafta, Z. Said, Impact of dust on the performance of solar photovoltaic (PV) systems under United Arab Emirates weather conditions,

Renew. Energy 141 (2019) 287–297, https://doi.org/10.1016/j.renene.2019.04.004.
[58] A.Y. Al-Hasan, A new correlation for direct beam solar radiation received by photovoltaic panel with sand dust accumulated on its surface, Sol. Energy 63 (1998) 323–333, https://doi.org/10.1016/S0038-092X(98)00060-7.
[59] M. Katoch, K. Kumar, V. Dahiya, Dust accumulation and reduction in electrical performance of solar PV panels, Mater. Today Proc. 46 (2020) 6608–6612, https://doi.org/10.1016/j.matpr.2021.04.082.
[60] H.A. Kazem, T. Khatib, K. Sopian, F. Buttinger, W. Elmenreich, A.S. Albusaidi, Effect of dust deposition on the performance of multi-crystalline photovoltaic modules based on experimental measurements, Int. J. Renew. Energy Resour. 3 (2013) 850–853.
[61] E. Klugmann-Radziemska, Degradation of electrical performance of a crystalline photovoltaic module due to dust deposition in northern Poland, Renew. Energy 78 (2015) 418–426, https://doi.org/10.1016/j.renene.2015.01.018.
[62] E. Klugmann-Radziemska, M. Rudnicka, The analysis of working parameters decrease in photovoltaic modules as a result of dust deposition, Energies 13 (2020), https://doi.org/10.3390/en13164138.
[63] A.K. Sisodia, R.K. Mathur, Performance analysis of photovoltaic module by dust deposition in western Rajasthan, Indian J. Sci. Technol. 13 (2020) 921–933, https://doi.org/10.17485/ijst/2020/v13i08/149928.
[64] P. Wang, J. Xie, L. Ni, L. Wan, K. Ou, L. Zheng, K. Sun, Reducing the effect of dust deposition on the generating efficiency of solar PV modules by super-hydrophobic films, Sol. Energy 169 (2018) 277–283, https://doi.org/10.1016/j.solener.2017.12.052.
[65] E. Zorn, T.R. Walter, Influence of volcanic tephra on photovoltaic (PV)-modules: an experimental study with application to the 2010 Eyjafjallajökull eruption, Iceland, J. Appl. Volcanol. 5 (2016), https://doi.org/10.1186/s13617-015-0041-y.
[66] J. Tanesab, M.D. Letik, A.A. Tino, Y.S. Peli, Experimental study of dust impact on power output degradation of various photovoltaic technologies deployed in West Timor, Indonesia, IOP Conf. Ser. Earth Environ. Sci. 188 (2018), https://doi.org/10.1088/1755-1315/188/1/012038.
[67] W. Yuan, Z. Liao, K. He, Q. Liu, S.M. Huang, An experimental investigation on condensation-induced self-cleaning of dust on superhydrophobic surface, Appl. Surf. Sci. 566 (2021) 150702, https://doi.org/10.1016/j.apsusc.2021.150702.
[68] Z.A. Darwish, K. Sopian, A. Fudholi, Reduced output of photovoltaic modules due to different types of dust particles, J. Clean. Prod. 280 (2021) 124317, https://doi.org/10.1016/j.jclepro.2020.124317.
[69] A. Hussain, A. Batra, R. Pachauri, An experimental study on effect of dust on power loss in solar photovoltaic module, Renewables Wind. Water, Sol. 4 (2017), https://doi.org/10.1186/s40807-017-0043-y.
[70] H. Lu, R. Cai, L.Z. Zhang, L. Lu, L. Zhang, Experimental investigation on deposition reduction of different types of dust on solar PV cells by self-cleaning coatings, Sol. Energy 206 (2020) 365–373, https://doi.org/10.1016/j.solener.2020.06.012.
[71] A.S. Shaharin, H.H. Haizatul, H.N.L. Nik Siti, S.I.R. Mohd, Effects of dust on the performance of PV panels, Int. J. Mech. Aerospace, Ind. Mechatron. Manuf. Eng. 5 (2011) 2028–2033, https://doi.org/10.5815/ijmecs.2012.10.04.
[72] B. He, H. Lu, Madina, Experimental study on the effect of dust deposition on the Output performance of photovoltaic modules, in: Int. Conf. Renew. Energies Smart Technol. REST 2022, IEEE, 2022, pp. 1–3, https://doi.org/10.1109/REST54687.2022.10022584.
[73] L. zhi Zhang, A. jian Pan, R. rong Cai, H. Lu, Indoor experiments of dust deposition reduction on solar cell covering glass by transparent super-hydrophobic coating with different tilt angles, Sol. Energy 188 (2019) 1146–1155, https://doi.org/10.1016/j.solener.2019.07.026.
[74] Y. Jiang, L. Lu, A study of dust accumulating process on solar photovoltaic modules with different surface temperatures, Energy Proc. 75 (2015) 337–342, https://doi.org/10.1016/j.egypro.2015.07.378.
[75] Y. Jiang, L. Lu, Experimentally investigating the effect of temperature differences in the particle deposition process on solar photovoltaic (PV) modules, Sustain. Times 8 (2016), https://doi.org/10.3390/su8111091.
[76] H. Lu, B. He, W. Zhao, Experimental study on the super-hydrophobic coating performance for solar photovoltaic modules at different wind directions, Sol. Energy 249 (2023) 725–733, https://doi.org/10.1016/j.solener.2022.12.023.
[77] A. Pan, H. Lu, L.Z. Zhang, Experimental investigation of dust deposition reduction on solar cell covering glass by different self-cleaning coatings, Energy 181 (2019) 645–653, https://doi.org/10.1016/j.energy.2019.05.223.
[78] M.Á. Muñoz-García, T. Fouris, E. Pilat, Analysis of the soiling effect under different conditions on different photovoltaic glasses and cells using an indoor soiling chamber, Renew. Energy 163 (2021) 1560–1568, https://doi.org/10.1016/j.renene.2020.10.027.
[79] K. Dastoori, G. Al-shabaan, M. Kolhe, D. Thompson, B. Makin, Impact of accumulated dust particles ' charge on the photovoltaic module performance, J. Electrostat. 79 (2016) 20–24, https://doi.org/10.1016/j.elstat.2015.11.006.
[80] S. Fan, Y. Wang, S. Cao, T. Sun, P. Liu, A novel method for analyzing the effect of dust accumulation on energy efficiency loss in photovoltaic (PV) system, Energy 234 (2021) 121112, https://doi.org/10.1016/j.energy.2021.121112.
[81] M. Al-Maghalseh, Experimental study to investigate the effect of dust, wind speed and temperature on the PV module performance, Jordan J. Mech. Ind. Eng. 12 (2018) 123–129.
[82] Z.S. Huang, C. Shen, L. Fan, X. Ye, X. Shi, H. Li, Y. Zhang, Y. Lai, Y.Y. Quan, Experimental investigation of the anti-soiling performances of different wettability of transparent coatings: superhydrophilic, hydrophilic, hydrophobic and superhydrophobic coatings, Sol. Energy Mater. Sol. Cells 225 (2021) 111053, https://doi.org/10.1016/j.solmat.2021.111053.
[83] Y.Y. Quan, L.Z. Zhang, Experimental investigation of the anti-dust effect of transparent hydrophobic coatings applied for solar cell covering glass, Sol. Energy Mater. Sol. Cells 160 (2017) 382–389, https://doi.org/10.1016/j.solmat.2016.10.043.
[84] P.G. Piedra, L.R. Llanza, H. Moosmüller, Optical losses of photovoltaic modules due to mineral dust deposition: experimental measurements and theoretical modeling, Sol. Energy 164 (2018) 160–173, https://doi.org/10.1016/j.solener.2018.02.030.
[85] S. Naz, M. Nadeem, M. Zain-Ul-Abideen, S.K. Buttar, S. Shukrullah, M.Y. Naz, Y. Jamil, Experimental investigation of impact of dust accumulation on the performance of photovoltaic solar module, IOP Conf. Ser. Mater. Sci. Eng. 863 (2020), https://doi.org/10.1088/1757-899X/863/1/012016.
[86] A.K. Tripathi, C.S.N. Murthy, M. Aruna, Experimental investigation on the influence of dust on PV panel performance and its surface temperature, Smart Syst. Green Energy. 1 (2018) 15–22, https://doi.org/10.23977/ssge.2018.11002.
[87] NASA, Material and Safety Datasheet, Mater. Saf. Datasheet, vols. 1–4, 2005. https://www.nasa.gov/sites/default/files/atoms/files/jsc-1a_material_safety_data_sheet.pdf. (Accessed 1 June 2023).
[88] S.A. Sulaiman, A.K. Singh, M.M.M. Mokhtar, M.A. Bou-Rabee, Influence of dirt accumulation on performance of PV panels, Energy Proc. 50 (2014) 50–56, https://doi.org/10.1016/j.egypro.2014.06.006.
[89] J. Chen, G. Pan, J. Ouyang, J. Ma, L. Fu, L. Zhang, Study on impacts of dust accumulation and rainfall on PV power reduction in East China, Energy 194 (2020) 116915, https://doi.org/10.1016/j.energy.2020.116915.
[90] M.S. El-Shobokshy, F.M. Hussein, Effect of dust with different physical properties on the performance of photovoltaic cells, Sol. Energy 51 (1993) 505–511, https://doi.org/10.1016/0038-092X(93)90135-B.
[91] Y. Wang, Methods for increasing the conversion efficiency of solar cells, J. Phys. Conf. Ser. 2221 (2022), https://doi.org/10.1088/1742-6596/2221/1/012040.
[92] H. Qasem, T.R. Betts, H. Müllejans, H. AlBusairi, R. Gottschalg, Effect of dust shading on photovoltaic modules, in: 26th Eur. Photovolt. Sol. Energy Conf. Exhib, 26th EU PVSEC), Hamburg, Germany, 2011.
[93] Central Microscopy Research Facility, Hitachi S-3400N, 2023. https://cmrf.research.uiowa.edu/hitachi-s-3400n. (Accessed 27 June 2023).
[94] Hitachi High-Technologies Corporation, S-3700N, 2023. https://www.hitachi-hightech.com/global/en/search/?ie=utf8&imgsize=0&q=S-3700N&input2=. (Accessed 27 June 2023).
[95] U. of M. LNF Wiki, Hitachi SU8000 In-Line FE-SEM, 2023. https://lnf-wiki.eecs.umich.edu/wiki/Hitachi_SU8000_In-line_FE-SEM. (Accessed 28 June 2023).
[96] IEN/IMat Materials Characterization Facility, Hitachi SU8010, 2023. https://mcf.gatech.edu/tools/hitachi-su8010/. (Accessed 28 June 2023).
[97] T. Ikegami, A. Yamaguchi, M. Tanaka, S. Takami, Y. Hojo, A. Sugimoto, Evolution and future of critical dimension measurement system for semiconductor processes, Hitachi Rev. 60 (2011) 203–209. http://128.241.23.25/rev/field/industriasystems/_icsFiles/afieldfile/2011/09/06/r2011_05_104.pdf.
[98] C.M.U, Materials Characterization Facility, Tescan Mira 3 FEG SEM, 2023. https://engineering.cmu.edu/mcf/equipment/tescan-mira-3.html. (Accessed 28 June 2023).
[99] C. and A.: T.U. of W.A. Centre for Microscopy, TESCAN VEGA3, 2023. https://www.cmca.uwa.edu.au/facilities/sem/tescan-vega3. (Accessed 28 June 2023).
[100] University of Missouri, Quanta 650 FEG, 2023. https://docs.research.missouri.edu/emc/FEI_Quanta_650FEG.pdf. (Accessed 28 June 2023).
[101] Max Planck Institute for Plant Breeding Research, Zeiss Supra 40VP, 2023. https://www.mpipz.mpg.de/4434223/zeiss-supra-40vp. (Accessed 28 June 2023).
[102] H. Menemmeche, M. Abderrezek, A. Ahriche, Performances of photovoltaic modules function in an aggressive environment, experimental study, J. Eng. Sci. Technol. Rev. 15 (2022) 60–66, https://doi.org/10.25103/jestr.154.09.
[103] L. Xu, S. Li, J. Jiang, T. Liu, H. Wu, J. Wang, X. Li, The influence of dust deposition on the temperature of soiling photovoltaic glass under lighting and windy conditions, Sol. Energy 199 (2020) 491–496, https://doi.org/10.1016/j.solener.2020.02.036.
[104] Z. Wu, S. Yan, T. Ming, X. Zhao, N. Zhang, Analysis and modeling of dust accumulation-composed spherical and cubic particles on PV module relative transmittance, Sustain. Energy Technol. Assessments 44 (2021), https://doi.org/10.1016/j.seta.2021.101015.
[105] M. Mazumder, M.N. Horenstein, J.W. Stark, P. Girouard, R. Sumner, B. Henderson, O. Sadder, I. Hidetaka, A.S. Biris, R. Sharma, Characterization of electrodynamic screen performance for dust removal from solar panels and solar hydrogen generators, IEEE Trans. Ind. Appl. 49 (2013) 1793–1800, https://doi.org/10.1109/TIA.2013.2258391.
[106] S. Sutha, S. Suresh, B. Raj, K.R. Ravi, Transparent alumina based superhydrophobic self–cleaning coatings for solar cell cover glass applications, Sol. Energy Mater. Sol. Cells 165 (2017) 128–137, https://doi.org/10.1016/j.solmat.2017.02.027.
[107] B. Guo, W. Javed, C. Pett, C.Y. Wu, J.R. Scheffe, Electrodynamic dust shield performance under simulated operating conditions for solar energy applications, Sol. Energy Mater. Sol. Cells 185 (2018) 80–85, https://doi.org/10.1016/j.solmat.2018.05.021.
[108] A. Al Shehri, B. Parrott, P. Carrasco, H. Al Saiari, I. Taie, Impact of dust deposition and brush-based dry cleaning on glass transmittance for PV modules applications, Sol. Energy 135 (2016) 317–324, https://doi.org/10.1016/j.solener.2016.06.005.

[109] SHIMADZU (Shimadzu Corporation, UV-2600i, 2023. https://www.shimadzu.com/an/products/molecular-spectroscopy/uv-vis/uv-vis-nir-spectroscopy/uv-2600i-uv-2700i/spec.html. (Accessed 28 June 2023).
[110] S. (Shimadzu Corporation), UV-3600, https://www.shimadzu.com/an/products/molecular-spectroscopy/uv-vis/uv-vis-nir-spectroscopy/uv-3600i-plus/spec.html, 2023. (Accessed 28 June 2023).
[111] PerkinElmer, LAMBDA 1050+ UV/Vis/NIR Spectrophotometer, 2023. https://www.perkinelmer.com/product/lambda-1050-2d-base-inst-no-sw-l6020055. (Accessed 28 June 2023).
[112] Ocean Insight, Spectrometers, 2023. https://www.oceaninsight.com/products/spectrometers/. (Accessed 28 June 2023).
[113] M.S. Mayhoub, A.A. Elqattan, A.S. Algendy, Experimental investigation of dust accumulation effect on the performance of tubular daylight guidance systems, Renew. Energy 169 (2021) 726–737, https://doi.org/10.1016/j.renene.2021.01.061.
[114] T. Rahman, A. Al Mansur, S. Islam, I. Islam, R. Awal, A. Shihavuddin, M. Asif, U. Haq, Effects of aging factors on PV modules output power : an experimental investigation, in: 4th Int. Conf. Sustain. Technol. Ind, vol. 4, IEEE, 2022, pp. 1–5, https://doi.org/10.1109/STI56238.2022.10103307, 0.
[115] H.A. Kazem, M.T. Chaichan, Effect of environmental variables on photovoltaic performance-based on experimental studies, Int. J. Civil, Mech. Energy Sci. 2 (2016) 1–8.
[116] A. Dajuma, S. Yahaya, S. Touré, A. Diedhiou, R. Adamou, A. Konaré, M. Sido, M. Golba, Sensitivity of solar photovoltaic panel efficiency to weather and dust over west Africa : comparative experimental study between niamey (Niger) and abidjan (côte d' ivoire), comput. Water, energy, Environ. Eng. 5 (2016) 123–147, https://doi.org/10.4236/cweee.2016.54012.
[117] A. Rao, R. Pillai, M. Mani, P. Ramamurthy, Influence of dust deposition on photovoltaic panel performance, Energy Proc. 54 (2014) 690–700, https://doi.org/10.1016/j.egypro.2014.07.310.
[118] W. Hu, X. Li, J. Wang, Z. Tian, B. Zhou, J. Wu, R. Li, W. Li, N. Ma, J. Kang, Y. Wang, J. Tian, J. Dai, Experimental research on the convective heat transfer coefficient of photovoltaic panel, Renew. Energy 185 (2022) 820–826, https://doi.org/10.1016/j.renene.2021.12.090.
[119] Mastech, Pocket Digital Multimeter M3900, 2023. https://mastech-group.com/na/en/M3900. (Accessed 29 June 2023).
[120] L. Sanwa, YX360TRF, Electric Instrument Co., 2023, https://overseas.sanwa-meter.co.jp/products/analog_multitester/yx360trf.html#specification. (Accessed 29 June 2023).
[121] Pro'sKit, MT-1210 Digital Multimeter, 2023. https://www.prokits.com.tw/Product/MT-1210/. (Accessed 29 June 2023).
[122] Eko, MP-160 I-V Tracer, 2023. https://www.eko-instruments.com/eu/categories/products/iv-measurement-instruments/mp-160-i-v-tracer. (Accessed 29 June 2023).
[123] IVIUM Technologies, IviumStat.H Standard, 2023. https://www.ivium.com/product/iviumstat-h-standard/. (Accessed 29 June 2023).
[124] MECO, 9009 Solar Module Analyzer, 2023. https://www.mecoinst.com/meco-product-details/Solar-Module-Analyzer.aspx. (Accessed 29 June 2023).
[125] PV Analyzers Prova. https://www.prova.com.tw/product_list.asp?seq=15#, 2023. (Accessed 29 June 2023).
[126] Hamburg Gunt, et al., 250 Solar Module Measurements, 2023. https://www.gunt.de/en/products/2e-energy/solar-energy/photovoltaics/solar-module-measurements/061.25000/et250/glct-1:pa-148:ca-669:pr-186. (Accessed 29 June 2023).
[127] Eternalsunspire, SPI-SUN 5600SLP BLUE Solar Simulator, 2023. https://eternalsunspire.com/product/tclf-aaa-single-long-pulse-temperature-controlled-lab-flasher/. (Accessed 29 June 2023).
[128] Circuit Specialists, Array 3711A Programmable DC Electronic Load, 2023. https://www.circuitspecialists.com/products/dc-electronic-load-csi3711a. (Accessed 29 June 2023).
[129] Tektronix, Keithley 2460 Source Measure Unit, 2023. https://www.tek.com/en/datasheet/2460-source-measure-unit. (Accessed 29 June 2023).
[130] Proskit, MT-1280 Digital Multimeter, 2023. https://www.prokits.com.tw/Product/MT-1280/. (Accessed 29 June 2023).
[131] Y. Andrea, T. Pogrebnaya, B. Kichonge, Effect of industrial dust deposition on photovoltaic module performance: experimental measurements in the tropical region, Int. J. Photoenergy 2019 (2019), https://doi.org/10.1155/2019/1892148.
[132] S. Liu, Q. Yue, K. Zhou, K. Sun, Effects of Particle concentration, deposition and accumulation on Photovoltaic device surface, Energy Proc. 158 (2019) 553–558, https://doi.org/10.1016/j.egypro.2019.01.151.
[133] Y. Guan, H. Zhang, B. Xiao, Z. Zhou, X. Yan, In-situ investigation of the effect of dust deposition on the performance of polycrystalline silicon photovoltaic modules, Renew. Energy 101 (2017) 1273–1284, https://doi.org/10.1016/j.renene.2016.10.009.
[134] Z. Wu, Z. Zhou, M. Alkahtani, Time-effective dust deposition analysis of PV modules based on finite element simulation for candidate site determination, IEEE Access 8 (2020) 65137–65147, https://doi.org/10.1109/ACCESS.2020.2985158.
[135] S. Oh, B.W. Figgis, S. Rashkeev, Effects of thermophoresis on dust accumulation on solar panels, Sol. Energy 211 (2020) 412–417, https://doi.org/10.1016/j.solener.2020.09.053.
[136] S.A. Sulaiman, H.H. Hussain, N. Siti, H.N. Leh, M.S.I. Razali, 3-studies-on-solar-PV-, 2011.
[137] P.G. Kale, K.K. Singh, C. Seth, Modeling effect of dust particles on performance parameters of the solar PV module, in: Fifth Int. Conf. Electr. Energy Syst, IEEE, 2019, pp. 1–5.
[138] LASI-1, Sciencetech Inc., 2023, https://www.sciencetech-inc.com/shop/product/165-9014-lasi-1-single-lasi-unit-5322?category=48. (Accessed 29 June 2023).
[139] Kipp, Zonen, Kipp & Zonen Pyranometers, Is an 11 Better than a 10? You Decide, - Kipp & Zonen, 2023. https://www.kippzonen.com/News/855/Kipp-Zonen-Pyranometers-is-an-11-better-than-a-10-You-decide. (Accessed 28 June 2023).
[140] G. Abal, A. Monetta, R. Alonso-Suárez, Outdoor solar radiometer calibration under ISO-9847:1992 standard and alternative methods, in: IEEE 9th Power, Instrum. Meas. Meet, EPIM, 2018, https://doi.org/10.1109/EPIM.2018.8756376, 2018.
[141] E. The Eppley Laboratory, Standard Precision Pyranometer, 2023. http://www.eppleylab.com/instrument-list/standard-precision-pyranometer/. (Accessed 28 June 2023).
[142] YSI, WE300 Pyranometer, 2023. https://www.ysi.com/we300. (Accessed 28 June 2023).
[143] TENMARS, Solar Power Meter, 2023. http://www.tenmars.com/m/2000-1682-19135.php?Lang=en. (Accessed 28 June 2023).
[144] CEM, DT-1307, https://www.cem-instruments.com/en/product-id-1311, 2023. (Accessed 28 June 2023).
[145] Ophir Photonics, Power Meters FAQ's, 2023. https://www.ophiropt.com/laser–measurement/knowledge-center/faq-pm. (Accessed 28 June 2023).
[146] A. Tilmatine, N. Kadous, K. Yanallah, Y. Bellebna, Z. Bendaoudi, A. Zouaghi, Experimental investigation of a new solar panels cleaning system using ionic wind produced by corona discharge, J. Electrostat. 124 (2023) 103827, https://doi.org/10.1016/j.elstat.2023.103827.
[147] Fritsch, Next Nano ANALYSETTE 22 Laser Particle Sizer, 2023. https://www.fritsch-international.com/particle-sizing/static-light-scattering/details/product/laser-particle-sizer-analysette-22-next-nano/. (Accessed 14 October 2023).
[148] Analytical Balance ME204 - Overview - METTLER TOLEDO, 2023. https://www.mt.com/be/en/home/products/Laboratory_Weighing_Solutions/analytical-balances/ME204.html. (Accessed 27 June 2023).
[149] Laboratory Balances & Scales, Lab Weighing METTLER TOLEDO, 2023. https://www.mt.com/be/en/home/products/Laboratory_Weighing_Solutions.html. (Accessed 27 June 2023).
[150] M. Li, B. Zhuang, Y. Lu, L. An, Z.-G. Wang, Supporting Information : Salt-Induced Liquid – Liquid Phase Separation : Combined Experimental and Theoretical Investigation of Water – Acetonitrile – Salt Mixtures, 2021.
[151] J. Polák, P. Morávek, Z. Brkljača, M. Vazdar, I. Cibulka, J. Heyda, Computation and volumetric insight into (p,T) effect on aqueous guanidinium chloride, J. Chem. Thermodyn. 158 (2021), https://doi.org/10.1016/j.jct.2021.106450.
[152] M. Saidan, A.G. Albaali, E. Alasis, J.K. Kaldellis, Experimental study on the effect of dust deposition on solar photovoltaic panels in desert environment, Renew. Energy 92 (2016) 499–505, https://doi.org/10.1016/j.renene.2016.02.031.
[153] M. Mani, R. Pillai, Impact of dust on solar photovoltaic (PV) performance: research status, challenges and recommendations, Renew. Sustain. Energy Rev. 14 (2010) 3124–3131, https://doi.org/10.1016/j.rser.2010.07.065.
[154] PAMAS, PAMAS OLS4031 Optical Particle Counter, 2023. https://www.pamas.de/particle-counters/products-by-name/pamas-ols4031. (Accessed 14 October 2023).
[155] W. Yao, X. Han, Y. Huang, Z. Zheng, Y. Wang, X. Wang, Analysis of the influencing factors of the dust on the surface of photovoltaic panels and its weakening law to solar radiation — a case study of Tianjin, Energy 256 (2022) 124669, https://doi.org/10.1016/j.energy.2022.124669.
[156] H.A. Kazem, M.T. Chaichan, A.H.A. Al-Waeli, A comparison of dust impacts on polycrystalline and monocrystalline solar photovoltaic performance: an outdoor experimental study, Environ. Sci. Pollut. Res. 29 (2022) 88788–88802, https://doi.org/10.1007/s11356-022-21958-5.
[157] K.S. AlZahrani, Experimental investigation of soiling impact on PV module performance in Yanbu Al Sinaiyah, Saudi Arabia, Renew. Energy 216 (2023) 119117, https://doi.org/10.1016/j.renene.2023.119117.
[158] A. Azouzoute, C. Hajjaj, H. Zitouni, M. El Ydrissi, O. Mertah, M. Garoum, A. Ghennioui, Modeling and experimental investigation of dust effect on glass cover PV module with fixed and tracking system under semi-arid climate, Sol. Energy Mater. Sol. Cells 230 (2021) 111219, https://doi.org/10.1016/j.solmat.2021.111219.